CUKUROVA UNIVERSITY

INSTITUTE OF NATURAL AND APPLIED SCIENCES

MSc THESIS

Effects of Phosphorus and Copper Based Catalysts on Nitrogen Oxides Conversion Performance of Hydrocarbon Selective Catalytic Reduction

Eylem Özgün ALICI

Automotive Engineering Department

November, 2024

CUKUROVA UNIVERSITY

INSTITUTE OF NATURAL AND APPLIED SCIENCES

MSc THESIS APPROVAL

Effects of Phosphorus and Copper Based Catalysts on Nitrogen Oxides Conversion Performance of Hydrocarbon Selective Catalytic Reduction

---

Eylem Özgün ALICI

Automotive Engineering Department

This Master's Thesis was evaluated by the following Jury Members on 08/11/2024 and was approved by unanimity / majority of votes.

Jury : Prof. Dr. Ali KESKIN (Advisor) ……

: Prof. Dr. Mustafa Atakan AKAR ……

: Assoc. Prof. Dr. Erinç ULUDAMAR ……

This Thesis was written in the Department of Automotive Engineering Institute of Natural and Applied Sciences.

Thesis Number:

Prof. Dr. Sadık DİNÇER
Director
Institute of Natural and Applied Sciences

CONTENTS

CUKUROVA UNIVERSITY
INSTITUTE OF NATURAL AND APPLIED SCIENCES

MSc THESIS

Effects of Phosphorus and Copper Based Catalysts on Nitrogen Oxides Conversion Performance of Hydrocarbon Selective Catalytic Reduction

Eylem Özgün ALICI

Advisor: Prof. Dr. Ali KESKİN

Department of Automotive Engineering

ABSTRACT

In this study, it was aimed to develop Phosphorus and Copper based catalysts for Hydrocarbon Selective Catalytic Reduction System and to determine the effect of these catalysts on NO_x conversions. Catalysts containing P(4%) /ZrO_2, P(3%)-Cu(1%)/ZrO_2, P(2%)-Cu(2%)/ZrO_2, P(1%)-Cu(3%)/ZrO_2, Cu(4%)/ZrO_2 were synthesised for HC-SCR system. Ethanol was used as reducing agent. SEM, XRD and BET analyses were performed to determine the structural and chemical properties of the catalysts. The catalysts were tested in the SCR system at a temperature range of 170°C-240°C and a constant field velocity of 40000 h^{-1}. The tests were carried out using a 2-cylinder V-type diesel engine at constant engine speed (3000 rpm) and under 3 different loads (0 kW, 2 kW and 4 kW). As a result, maximum NO_x conversion rates were measured for 3P1CZ at 4 kW load, 240 °C temperature, 40000 h^{-1} gas hourly space velocity.

Keywords: SCR, NO_x, Diesel Engine Emission, Catalyst

ÇUKUROVA ÜNİVERSİTESİ
FEN BİLİMLERİ ENSTİTÜSÜ

YÜKSEK LİSANS TEZİ

Fosfor ve Bakır Bazlı Katalizörlerin Hidrokarbon Seçici Katalitik İndirgemenin Azot Oksit Dönüşüm Performansı Üzerindeki Etkileri

Eylem Özgün ALICI

Danışman: Prof. Dr. Ali KESKİN

Otomotiv Mühendisliği Anabilim Dalı

ÖZ

Bu çalışmada, Hidrokarbon Seçici Katalitik İndirgeme Sistemi için Fosfor ve Bakır bazlı katalizörlerin geliştirilmesi ve bu katalizörlerin NO_x dönüşümleri üzerindeki etkisinin tespit edilmesi amaçlanmıştır. HC-SCR sistemi için P(4%) / ZrO_2, P(3%)-Cu(1%) / ZrO_2, P(2%)-Cu(2%) / ZrO_2, P(1%)-Cu(3%)/ ZrO_2, Cu(4%)/ ZrO_2 içerikli katalizörler sentezlenmiştir. İndirgeyici malzeme olarak etanol kullanılmıştır. Katalizörler ait yapısal ve kimyasal özellikleri belirlemek amacıyla SEM, XRD ve BET analizleri gerçekleştirilmiştir. Katalizörler 170°C-240°C sıcaklık aralığında ve 40000 h^{-1} sabit alan hızında SCR sisteminde test edilmiştir. Testler 2 silindirli V-tipi bir dizel motor kullanılarak sabit motor devrinde (3000 devir/dakika) ve 3 farklı yük (0 kW, 2 kW ve 4 kW) altında gerçekleştirilmiştir. Sonuç olarak, maksimum NO_x dönüşüm oranları 3P1CZ katalistinde 4 kW yükte, 240 ℃ sıcaklıkta, 40000 h^{-1} gaz saatlik alan hızında ölçülmüştür.

Anahtar Kelimeler: SCR, NO_x, Dizel Motor Emisyonu, Katalist

GENİŞLETİLMİŞ ÖZET

Dünya çok sayıda çevre sorunuyla karşı karşıyadır ve gaz emisyonlarının neden olduğu kirliliğin azaltılması zorunlu hale gelmektedir. Kirleticiler çoğunlukla termik santrallerden, kimyasal üretim tesislerinden, otomobillerden ve dizel motorlardan kaynaklanmaktadır. Fosil yakıtların yenilenebilir enerji ile değiştirilmesi için çeşitli çabalar sarf edilmiştir, ancak 2018 itibariyle elektriğin %61' i hala fosil yakıtların yakılmasıyla üretilmektedir. Kirli hava kabul edilemez seviyelerde karbondioksit (CO_2), karbon monoksit (CO), sülfür oksitler (SO_x), azot oksitler (NO_x), partikül madde (PM) ve uçucu organik bileşikler (VOC' ler) içermektedir.

Dizel motorların birçok avantaja sahip olması nedeniyle otomotiv sektöründe ve endüstriyel alanlarda yaygın olarak kullanılmaktadır. Bu nedenle kullanımda olan dizel motorların sayısı oldukça artmıştır. Kaynakların kullanımları sırasında sağladıkları avantajların yanı sıra çeşitli dezavantajları da beraberinde getirmektedir. Dizel motorların enerji verimliliğinin yanı sıra en önemli dezavantajı, çalışmaları sırasında çevreye yaydıkları emisyonlardır. İçten yanmalı motorlardan yayılan azot oksitler (NO_x) ve partikül madde gibi zararlı kirleticiler hava kalitesi ve insan sağlığı için son derece zararlıdır. Azot oksitlerin atmosferde nitrik asite (HNO_3) dönüşmesi sonucunda asit yağmurlarının oluşumu tetiklenir. Azot dioksitin, ortamlarda ozon ve diğer kirleticilerle etkileşime girmesi sonucu oluşan tepkimeler, insan sağlığını tehdit eden etmenler doğurur.

Son yıllarda, içten yanmalı motorların yanma öncesi ve sonrası aşamalarında araç emisyonlarını kontrol etmek için çok sayıda emisyon kontrol tekniği araştırılmıştır. Azot oksitlerin çevre üzerindeki artan zararlı etkisi nedeniyle, azot oksit emisyonlarının kontrolü için emisyon yönetmelikleri sıkı bir şekilde güncellenmektedir. Bu sıkı gereklilikler sadece yeniden formüle edilmiş yakıt veya yanma olaylarıyla karşılanamaz. Yoğun bir son işlem teknolojisi gerektirecektir. Üç yollu katalitik konvertörler, LNT ve SNCR tabanlı azot oksit azaltma teknolojileri arasında seçici katalitik indirgeme sistemi, hafif ve ağır hizmet araçlarında azot oksit emisyonlarını %90' a kadar kontrol etmede önemli bir potansiyele sahiptir. Geliştirilmiş bir seçici katalitik indirgeme teknolojisi için mevcut pazar potansiyeli nedeniyle, üstün katalist teknolojisi, gelişmiş indirgeyici dozajlama stratejisi ve yan ürün sınırlaması gibi seçici katalitik indirgeme sistemini optimize etmek için birçok çaba sarf edilmiştir.

NO_x emisyonlarının azaltması için en etkili yöntem seçici katalitik indirgeyici (SCR) sistemidir. Bu sistemde bir indirgeyici vasıtasıyla NO_x emisyonları, su ve azota (N_2) dönüştürülmektedir. SCR sisteminde indirgeyici malzeme olarak amonyak ya da etanol kullanılmaktadır. Bu sistem NH_3-SCR olarak adlandırılır. Bu teknolojiye ek olarak düşük sıcaklıklarda da kullanılmaya uygun olan HC-SCR (Hidrokarbon SCR) sistemleri üzerine de birçok çalışma yapılmaktadır. Etanol, metanol, propanol gibi hidrokarbonların SCR sisteminde kullanılmasıyla NO_x dönüşüm oranında artış gözlemlenmektedir.

SCR sisteminde kullanılan katalistler farklı metal katkılarıyla daha iyi performans göstermektedir. Ag (gümüş), Fe (Demir), Ce (Seryum), Cu (Bakır), V (Vanadium), P (Fosfor) Pt (Platin) vb. metallerini içeren katalizörler kullanılmaktadır.

Bu çalışma kapsamında NO_x emisyonunu azaltmak amaçlı Hidrokarbon Seçici Katalitik İndirgeme Sisteminde (HC-SCR) kullanılmak üzere P-Cu-ZrO_2; esaslı katalizörler absorpsiyon yöntemiyle sentezlenmiştir. Farklı oranlarda fosfor ve bakır ilavesi ile zirkonyum dioksit bazlı 5 katalist üretilmiştir; 4PZ, 3P1CZ, 2P2CZ, 1P3CZ, 4CZ. Üretilen katalizörlerin test düzeneğinde etanol ilavesi yapılarak, dizel motordan yayılan NO_x emisyonunun dönüşüm oranına etkisi incelenmiştir.

Katalizör üretimi amacıyla 400 cpsi kare gözeneğe sahip olan kordiyerit ($2Al_2O_3 – 5SiO_2 – 2MgO$) tek parça ana taşıyıcı yapı kullanılmıştır. Kordiyerit malzeme, kaplama işleminden önce kaplanacak olan yüzeyin yüzey alanını arttırmak amacıyla her bir numune için 250 gram oksalik asit ve 500 ml saf su karışımı ile ön işleme tabi tutulmuştur. Bu ön işlem 90 °C sıcaklıkta 4 saat boyunca uygulanmıştır. Ön işlem tamamlanarak kordiyerit malzeme kaplama prosesi için hazır hale getirilmiştir. Karışım hazırlamak amacıyla 5.72 gram ($(NH_4)H_2PO_4$), 4.973 gram (Cu $(NO_3)_2 3H_2O$) kullanılmıştır. Elde edilen karışım 300 ml saf suya karıştırılmıştır. Bu karışım 1 saat boyunca ultrasonik karıştırıcı yardımıyla tekrar karıştırılmıştır. Daha sonra karışımın içerisine bağlayıcılığı artırmak amacıyla; toz katalistin ağırlıkça %1'i kadar SiO_2 eklenerek karıştırmaya devam edilmiştir. Elde edilen karışım 90 ℃ sıcaklıkta içerisindeki su buharlaşıncaya kadar ultrasonik karıştırıcı yardımıyla karıştırılmıştır. Daha sonra karışım içerisindeki suyun tamamen buharlaşması amacıyla 110 ℃ sıcaklıkta 1 saat fırınlanmıştır. Fırından alınan karışım 550 ℃ sıcaklıkta 2 saat kalsine edilmiştir. P, Cu ve Zr partiküllerini içeren toz haline getirilen karışımdan 40 gram alınarak 400 mililitre saf su ile tekrar karışım hazırlanmıştır. Bu karışımın içerisine kordiyerit malzeme daldırılarak kaplama işlemine başlanmıştır. Daldırma işlemi her bir katalist için 3 kez tekrarlanmıştır. Sonrasında kordiyerit malzeme 120 ℃ sıcaklıkta 1 saat süresince fırında kurutulup, ardından 550 ℃ sıcaklıkta 3 saat kalsine edilmiştir. Bu işlemlerin sonunda katalist üretimi tamamlanmıştır.

Üretimi tamamlanan katalizörün SEM, XRD ve BET analizleri yapılarak kimyasal ve yapısal özellikleri ortaya çıkarılmıştır. Oluşturulan HC-SCR sisteminde indirgeyici olarak etanol kullanılmıştır. Elde edilen katalizörlerin gerçek dizel egzoz gazına maruz bırakılması ile NO_x dönüşüm oranları ölçülmüştür.

Üretilen katalizörler; Çukurova Üniversitesi Otomotiv Mühendisliği Bölümü Laboratuvarlarında kurulan SCR egzoz performans test sisteminde bir dizi teste tabi tutulmuştur. Test esnasında 2 silindirli V tipi dizel motor kullanılmıştır. Gerçek emisyon gazı kullanarak 40000 h^{-1} sabit alan hızında, 170-240 °C sıcaklık aralığında ve 3 farklı motor yükünde (0 kW, 2 kW, 4 kW) yapılmıştır. Egzoz gazındaki sıcaklık artışının NO_x dönüşüm verimliliğini artırdığı gözlemlenmiştir. Test edilen 3 farklı motor yükünde ise en fazla NO_x dönüşüm oranı en yüksek motor yükü olan 4 kW' da gözlemlenmiştir. P ve Cu bazlı katalizörlerin NO_x dönüşüm oranlarını karşılaştırmak

gerekirse; fosforun ağırlıkça fazla olduğu katalistlerde daha yüksek oranda NO_x dönüşümü gözlemlenmiştir. Bakır içeriğinin artması ile birlikte dönüşüm oranlarında azalma gözlemlenmiştir.

ACKNOWLEDGEMENTS

First of all, I would like to thank my supervisor Prof. Dr. Ali KESKİN for his support and encouragement throughout the preparation of this thesis.

I would also like to thank Research Assistant Ali Cem YAKARYILMAZ, for his generosity with his time and constant help that I needed especially during the research and writing and for his great support during all the experiments.

I would like to thank my classmate Research Assistant Berkay KARAÇOR for his moral support and kindness.

I would like to thank to all Automotive Engineering Department academic personals for their support.

Finally, I also would like to thank my family for their support throughout my master's studies and the preparation of this thesis. Their encouragement has been the most important factor in my completion of this thesis. Even at times when I lost confidence in myself, they continued to encourage me. Thank you very much!

LIST OF TABLES

LIST OF FIGURES

SYMBOLS AND ABBREVIATIONS

kW	: Kilowatt
W	: Watt
kV	: Kilovolt
V	: Volt
ppm	: Parts per million
m	: Meter
Cm	: Centimeter
mm	: Millimeter
nm	: Nanometer
lt	: Liter
ml	: Milliliter
cpsi	: Cells per square inch
hPa	: Hectopascal
g	: Gram
hr	: Hour
min	: Minute
s	: Second
K	: Kelvin
F	: Fahrenheit
C	: Celsius
wt	: Weight
vol	: Volume
RPM	: Revolution per minute
SCR	: Selective Catalytic Reduction
HC	: Hydrocarbon
NO_x	: Nitrogen Oxides
SEM	: Scanning Electron Microscopy
BET	: Branauer – Emmet – Teller
XRD	: X-Ray Diffraction
XRF	: X-Ray Fluorescence
PM	: Particulate Matter
PN	: Particulate Number
DPF	: Diesel Particulate Filter
DOC	: Diesel Oxidation Catalyst

LNT	: Lean NO_x Trap
EGR	: Exhaust Gas Recirculation
SO_X	: Sulfur Oxides
ECE	: Economic Commission for Europe
ESC	: European Stationary Cycle
ELR	: European Load Response
WHSC	: World Harmonized Stationary Cycle
WHTC	: World Harmonized Transient Cycle
TWC	: Three-Way Catalytic Convertor
CAS	: Chemical Abstracts Service
CO_2	: Carbon Dioxide
CO	: Carbon Monoxide
NO	: Nitric Oxide
NO_2	: Nitrogen Dioxide
NO_3	: Nitrate
OH	: Hydroxide
SOF	: Soluble Organic Fraction
Al_2O_3	: Aluminium Oxide
CeO_2	: Cerium Dioxide
ZrO_2	: Zirconium Dioxide
$(Cu(NO_3)_2x3H_2O)$	: Copper (II) Nitrate Trihydrate
$(C_2H_2O_4)$	: Oxalic Acid
NH_3	: Ammonia
µm	: Micrometer
P	: Phosphorus
Cu	: Copper
VOCs	: Volatile Organic Compounds
HNO_3	: Nitric Acid
SNCR	: Selective non catalytic reduction
Ag	: Silver
Fe	: Iron
V	: Vanadium
Ce	: Cerium
Pt	: Platinum
SiO_2	: Silicon Dioxide
EU	: European Union
EC	: European Council
NMOG	: Non-Methane Organic Gases
LPG	: Liquefied Petroleum Gas

THC : Total Hydrocarbons
DeNOx : Denitrification
ZSM : Zeolite Secony Mobil

1. INTRODUCTION

The world is grappling with numerous environmental issues, and it is increasingly imperative to cut down on pollution from gaseous emissions. Thermal power plants, chemical production facilities, motor vehicles, and diesel engines are the primary sources of pollutants. Despite various initiatives to replace fossil fuels with renewable energy sources, as of 2018, 61% of global electricity generation still depended on burning fossil fuels, such as coal, natural gas, and oil. Prevailing atmospheric conditions have been identified as significant contributors to environmental degradation, with elevated levels of carbon dioxide (CO_2), carbon monoxide (CO), sulfur oxides (SO_x), nitrogen oxides (NO_x), particulate matter (PM), and volatile organic compounds (VOCs) being observed (Asghar et al., 2021).

The diesel engine is the primary source of power for a vast array of heavy-duty machinery, including ships, trains, agricultural tractors, buses, and, for the past five decades, passenger cars. Most notably, diesel offers a highly efficient and flexible utilization of fuel, coupled with a high energy density. Additionally, it exhibits superior capabilities for storage and distribution. The engine manufacturers are keenly aware of the imperative for environmental responsibility and the need to address the challenges posed by individual mobility. The engine is designed to run on a range of alternative fuel sources. Over the past two and a half decades, significant advancements have been made with regard to the emission of NO_x, smoke, unburned oil and noise (Lakshminarayanan, 2020).

Many vehicles on the road have significantly decreased their NO_x emissions, sometimes by as much as 80%, by implementing relatively straightforward software updates. This success can be attributed to the extensive expertise and understanding of Selective Catalytic Reduction (SCR) in the automotive industry. In nations with stringent emission regulations, there has been a reduction of over 70% in NO_x pollution since 1990. It's important to note that real driving cycle (RDE) emissions exceed laboratory measurements. However, it is expected that within the next five years, there will be a 90% reduction from current levels. The integration of the new generation fuel injection systems with SCR and mild hybrid options such as start-stop, e-turbochargers promises notable enhancements in fuel consumption and emissions (Lakshminarayanan, 2020).

2. DIESEL ENGINE EMISSIONS AND EMISSION CONTROL SYSTEMS

2.1. Diesel Engine Emissions

The emissions generated by internal combustion engines encompass hydrocarbons (HC), carbon monoxide (CO), oxides of nitrogen (NO_x), and particulate matter. Hydrocarbons denote unburned fuel molecules that give rise to smaller, non-equilibrium particles. Incomplete combustion due to insufficient oxygen or incomplete air-fuel mixing results in the production of carbon monoxide. Oxides of nitrogen form at high combustion temperatures due to the dissociation of stable nitrogen and subsequent combination with reacting oxygen. Particulate matter, evident as black smoke from compression ignition engines, is another combustion byproduct. Additional emissions present in engine exhaust include aldehydes, sulfur, lead, and phosphorus (Pulkrabek et al.,2004).

2.1.1. Oxides of Nitrogen (NO_x)

It is well-established that nitrogen oxide (NO_x) emissions, comprising nitric oxide (NO) and nitrogen dioxide (NO_2), represent a substantial source of atmospheric pollution. Such activities have a detrimental impact on the environment and human health. The main environmental impacts of NO_x include acidification of precipitation, the formation of photochemical smog, the greenhouse effect and ozone depletion. It is widely acknowledged that the most severe human health effect of NO_x is respiratory tract disease (Aswin et al., 2022).

Diesel vehicles represent a significant source of NO_x emissions. In combustion processes, NO_x is composed partly of nitrogen compounds present in the fuel, including ammonia (NH_3), nitric acid (HCN), and nitrogen oxides (NO_x). However, NO_x primarily results from the direct combination of oxygen from the atmosphere with nitrogen present in the combustion flame and is emitted from the exhaust as an unwanted byproduct. The formation of NO_x emissions can be classified into three categories: fuel, prompt, and thermal. The formation of fuel NO_x occurs when nitrogen compounds present in the fuel react with atmospheric oxygen. The resulting NO_x is formed because of the reaction between hydrocarbon free radicals, which are produced during the initial stages of the combustion process, and molecular nitrogen. This reaction is known as prompt NO_x formation. The formation of thermal NO_x can take place when nitrogen and oxygen present in the air interact under high temperatures (Özarslan, 2022; Shan et al., 2020).

2.1.2. Hydrocarbons (HC)

Hydrocarbons and carbon monoxide (CO) make up the second component of diesel exhaust. Alkanes, alkenes and aromatics are the main classes of hydrocarbons. Although the toxicity, carcinogenicity and effect on oxidation formation of these compounds may vary between species, they are collectively referred to as Total Hydrocarbons (THC) (Yamada et al., 2011).

Diesel engines have lower HC emissions than gasoline engines. This is because they run on a completely lean mixture. The high molecular weight of diesel fuel components results in elevated boiling and condensing temperatures. This allows some HC particles to condense on the solid carbon surface formed when burning. Most of these particles are burned as the mixture and combustion process continues. Only a small portion of this carbon soot is expelled from the cylinder through the exhaust pipe. Condensation of HCs on the carbon surface leads to HC emissions in the engine (Pulkrabek, 2004).

The combustion efficiency of a diesel engine is typically around 98%, with only approximately 2% of the HC fuel present in the exhaust as an emission. In the cylinder, there will be regions of poor mixing, where the combustion process is not optimally initiated and sustained. Additionally, there will be regions of excessively rich mixing, where the lack of oxygen precludes complete combustion of the entire mixture. Incomplete combustion may be attributed to the heterogeneous mixture. In diesel engines, the range of mixture zones, from very rich to very poor, is considerable, and the formation of multiple flame fronts is a further characteristic. As a consequence of the inadequate mixture, some fuel particles in the rich mixture zones are unable to locate oxygen for reaction. A portion of the fuel may remain unburned due to the limitation of combustion in lean mixture areas. In the event of an excessive mixture, some fuel particles may not undergo complete combustion due to their mixing with burnt gases. Consequently, HC emissions are observed in diesel engines. In diesel engines, the fuel properties, injectors, crevice volume, oil film absorption, and wall deposit absorption are factors that influence hydrocarbon emissions (Özarslan, 2022).

2.1.3. Particulate Matter (PM)

Particulate matter (PM) emissions in exhaust gases are a consequence of the combustion process. It is believed that the formation of particulate matter is due to the aggregation of a number of factors, including partially burnt fuel, partially burnt lubricating oil, ash content of fuel, cylinder lubricating oil, sulfate and water (Reşitoğlu, 2016).

The diesel aftertreatment system is evolving rapidly, comprising an oxidation catalyst, a diesel particulate filter (DPF), and a NO_x reduction strategy. The composition of PM is influenced by each of these components. It should be noted that the catalyst itself does not specifically reduce PM emissions. However, it may contribute to this indirectly by influencing the precursors of semi-volatile PM. Additionally, research has demonstrated that the oxidation of SO_2 to SO_3 results in an accelerated formation of nucleation mode particles. (Maricq, 2007).

It is a well-documented fact that the emissions of particulate matter produced by diesel engines are significantly higher than those emitted by gasoline engines. It is possible to classify emissions of diesel particles according to three main categories: soot, the soluble organic fraction (SOF), and the inorganic fraction (IF). It is notable that over 50% of total PM emissions are constituted by soot, which is defined as visible black smoke. SOF, or sulfur oxides, comprises heavy

hydrocarbons that are adsorbed or condensed onto the soot. It can be derived from lubricating oil, unburned fuel and also from the formation of compounds during combustion. SOF levels tend to be higher in situations where there is a low engine load, coupled with low exhaust temperatures (Sarvi et al., 2011; Reşitoğlu et al., 2014).

A number of adverse health outcomes have been linked to PM emissions. The aforementioned adverse health outcomes appear to include an elevated risk of developing lung cancer, asthma, bronchitis, and cardiovascular and respiratory diseases. Furthermore, these emissions cause environmental contamination, particularly of water, soil, and air (Özarslan, 2022; Reşitoğlu et al., 2014).

2.1.4. Carbon Monoxide (CO)

Carbon monoxide (CO), a colorless, odorless, toxic gas, is produced when an engine operates with an excess of fuel relative to air. When insufficient oxygen is available to fully oxidize the carbon, incomplete combustion occurs, resulting in the formation of CO. Typically, the exhaust of a spark-ignited (SI) engine will contain approximately 0.2% to 5% carbon monoxide. It is important to note that carbon monoxide is not merely an undesirable emission; it also represents the loss of potential chemically stored energy within the engine that was not able to be accessed and utilized due to the presence of this emission. This substance, which is a fuel in its own right, can be combusted in order to generate additional thermal energy (Pulkrabek, 2004).

$$CO + ½\ O_2 \rightarrow CO_2 + \text{heat}$$

The CO formation during the combustion of a hydrocarbon radical “R” in a diesel engine is shown in reaction as follows.

$$RH \rightarrow R \rightarrow RO_2 \rightarrow RCHO \rightarrow RCO \rightarrow RC$$

As seen in the reaction above, hydrocarbon radical transforms to the CO.
Then CO slowly oxidizes to CO_2 as like in the reactions below (Çalışkan, 2021).

$$CO + O_2 \rightarrow CO_2 + O$$

$$O + H_2O \rightarrow 2OH$$

$$CO + OH \rightarrow CO_2 + H$$

$$H + O2 \rightarrow OH + O$$

2.2. Diesel Engine Emission Regulations

It is widely acknowledged that pollution represents a significant threat to human life and the natural ecosystems on which we depend. Pollution represents the greatest environmental risk factor for the prevalence of psychological and physical health issues, as well as increased mortality rates, which are notably higher among children, people with specific health problems. In addition to its impact on human health, pollution is a primary driver of biodiversity loss. It impairs the capacity of ecosystems to provide essential services such as carbon sequestration and decontamination. The imperative for the EU to lead the global effort against pollution is now more compelling than ever, based on considerations of public health, the environment, morality, and socio-economic factors (EU Commission, Zero Pollution Action Plan).

According to regulation (EU) 2024/1257:

> "The technical requirements for the type-approval of motor vehicles, engines and replacement parts with regard to emissions are currently set out in two Regulations that apply to emission type-approval for light-duty and heavy-duty vehicles respectively, namely Regulation (EC) No 715/2007 of the European Parliament and of the Council and Regulation (EC) No 595/2009 of the European Parliament and of the Council. the current emission limits for heavy-duty vehicles were adopted in 2009 on the basis of the available technology at that time. Since then, technology has advanced and the level of emissions achievable with a combination of current technologies is much lower than that achievable more than 15 years ago. That technological progress should be reflected in emission limits based on existing state-of-the-art technology and knowledge of pollution controls and for all relevant pollutants. Regulations (EC) No 715/2007 and (EC) No 595/2009 require that vehicles respect the emission limits for a specified period of time, which does not correspond to the average lifetime of vehicles. It is therefore appropriate to lay down durability requirements that reflect the average expected lifetime of vehicles in the Union" (EUR-Lex, (EU) 2024/1257).

Table 2.1. EU emission standards for heavy-duty CI (diesel) engines: Steady-state testing (Dieselnet, Emission Standards).

Stage	Date	Test	CO	HC	CH_4	NOx	NH_3	N_2O	PM	PN	Smoke
			g/kWh							*1/kWh*	*1/m*
Euro I	1992, ≤ 85 kW	ECE R-49	4.5	1.1		8.0			0.612		
	1992, > 85 kW		4.5	1.1		8.0			0.36		
Euro II	1996.10		4.0	1.1		7.0			0.25		
	1998.10		4.0	1.1		7.0			0.15		
Euro III	*1999.10 EEV only*	ESC & ELR	*1.5*	*0.25*		*2.0*			*0.02*		*0.15*
	2000.10		2.1	0.66		5.0			0.10[a]		0.8
Euro IV	2005.10		1.5	0.46		3.5			0.02		0.5
Euro V	2008.10		1.5	0.46		2.0			0.02		0.5
Euro VI	2013.01	WHSC	1.5	0.13		0.40	10 ppm		0.01	8.0×10^{11}[b]	
Euro VII	2028.05.29		1.5	0.080[d]	0.5	0.200	0.060	0.20	0.008	6.0×10^{11}[c]	

[a] PM = 0.13 g/kWh for engines < 0.75 dm^3 swept volume per cylinder and a rated power speed > 3000 min^{-1}
[b] PN_{23}
[c] PN_{10}
[d] NMOG

Table 2.2. Euro 7 exhaust emission limits for vehicles of categories M2, M3, N2 and N3 (Dieselnet, Emission Standards).

Stage	Date	Test	CO	NMHC	CH_4[a]	NOx	NH_3	N_2O	PM[b]	PN
			g/kWh							*1/kWh*
Euro III	1999.10 EEV only	ETC	3.0	0.40	0.65	2.0			0.02	
	2000.10		5.45	0.78	1.6	5.0			0.16[c]	
Euro IV	2005.10		4.0	0.55	1.1	3.5			0.03	
Euro V	2008.10		4.0	0.55	1.1	2.0			0.03	
Euro VI	2013.01	WHTC	4.0	0.16d	0.5	0.46	10 ppm		0.01	6.0×1011e
Euro VII	2028.05.29		1.5	0.080[g]	0.5	0.200	0.060	0.200	0.008	6.0×10^{11}[f]

[a] Euro III-V: NG only; Euro VI: NG + LPG; Euro VII: all engines
[b] not applicable for gas fueled engines at the Euro III-IV stages
[c] PM = 0.21 g/kWh for engines < 0.75 dm3 swept volume per cylinder and a rated power speed > 3000 min-1
[d] THC for diesel (CI) engines
[e] PN23. PN limit for PI engines applies for Euro VI-B and later [EC 2014]
[f] PN10
[g] NMOG

2.3. Diesel Engine Emission Control Systems

Emission standards obligate manufacturers to produce sophisticated technologies, including diesel particulate filters (DPFs), diesel oxidation catalysts (DOCs), exhaust gas recirculation (EGR) systems, lean NO_x arrestors (LNTs), three-way catalytic converters (TWC), and selective catalytic reduction (SCR) systems, which are employed to mitigate diesel engine emissions. This section will provide an in-depth examination of the exhaust emission reduction systems that have been developed as a result of extensive research and analysis (Çalışkan, 2021).

2.3.1. Diesel Oxidation Catalyst (DOC)

The use of diesel oxidation catalysts enables the conversion of carbon monoxide (CO) and hydrocarbons (HC) into carbon dioxide (CO_2) and water. This process effectively reduces the overall quantity of diesel combustion particulates emitted into the atmosphere. However, they demonstrate minimal impact on nitrogen oxides (NO_x). An oxidation catalyst can effectively remove up to 90% of the soluble organic fraction (SOF) of diesel particulate matter, offering a highly effective solution for reducing emissions. Given the considerable number of chemicals present in this section of the particle, it is of paramount importance to eliminate SOF, which has been identified by health experts

as a significant cause for concern. A Furthermore, DOCs are utilized in a combined approach with NO_x adsorbers, $DeNO_x$ catalysts, DPFs, or selective catalytic reduction (SCR) in order to elevate NO_2 emission levels or to "clean up" any bypass of injection of reductant employed for NO_x reduction (Keskin and Emiroğlu, 2016).

The system functions by reacting harmful gases released from the exhaust with harmless gases, such as CO and HC, in the environment. This reaction is facilitated by a catalyst. The gases' flow direction is typically longitudinal. A palladium or platinum coating is added to the catalytic feature, which is a metallic or ceramic honeycomb structure. As a result, CO and HC gases are converted to water and carbon dioxide. However, the system does not reduce NO_x, and its effect on NO_x allows NO and NO_2 to be proportionally equal. This contributes to the SCR system's overall efficiency (Özarslan, 2022).

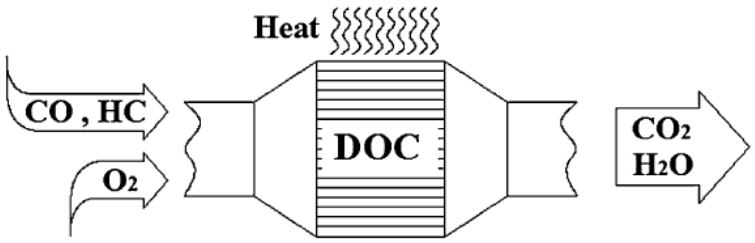

Figure 2.1. Diesel oxidation catalyst (DOC) (Reşitoğlu et al., 2015).

Reactions in DOC system (Zheng and Banerjee, 2009):

$$CO + ½\ O_2 \rightarrow CO_2$$
$$C_3H_6 + 9/2\ O_2 \rightarrow 3\ CO_2 + 3H_2O$$
$$CnHm + (n+m/4)\ O_2 \rightarrow nCO_2 + m/2H_2O$$
$$NO + ½\ O_2 \rightarrow NO_2$$

2.3.2. Diesel Particulate Filter (DPF)

Diesel particulate filters (DPFs) are devices that utilize filtration processes to physically capture diesel particulates, thereby preventing their release into the atmosphere. It has been demonstrated that DPFs are an adequate technology for the control of particle mass and number. The filtration process of these devices is most optimal when controlling the solid composition of diesel particulates. These include elemental carbon (soot) and the associated black smoke emissions. It is conceivable that filters may exhibit diminished efficacy or even complete ineffectiveness in regulating non-solid components of PM emissions, particularly the organic fraction (OF) and sulfate particulates. In order to regulate the totality of PM emissions, the majority of DPF systems incorporate catalysts that facilitate the oxidation of the organic fraction (OF). The use of ultra-low

sulfur fuels is also a necessity to enable the use of catalysts and to control sulfate particulates (Dieselnet, Diesel Particulate Filters; Majewski, 2020).

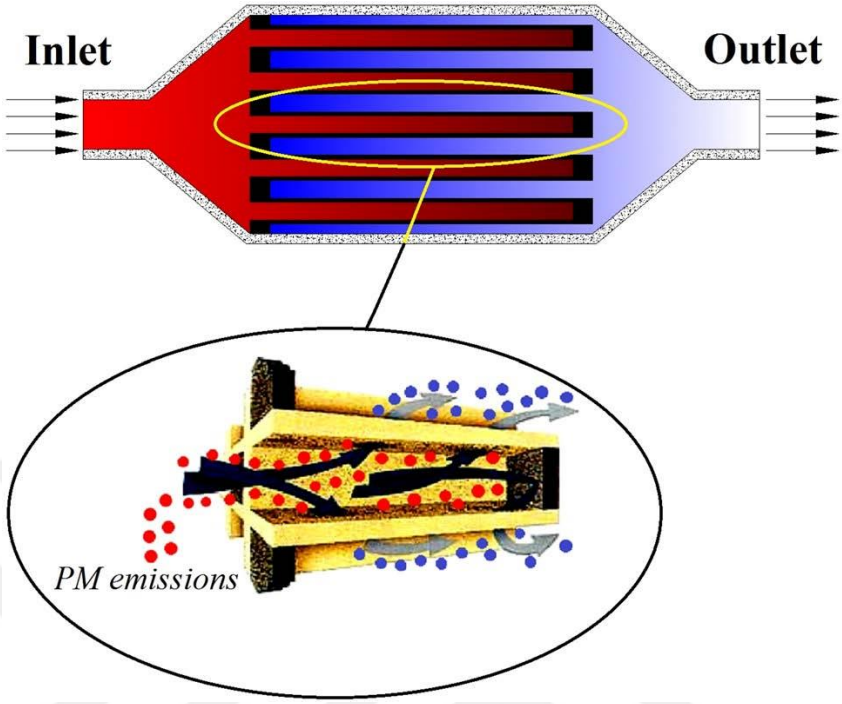

Figure 2.2. Diesel Particulate Filter (DPF) (Reşitoğlu et al.).

The selection of DPF materials is based on a number of factors, including high temperature resistance, extreme resistance to thermal stresses, corrosion resistance, and mechanical strength characteristics. DPFs are typically manufactured using silicon carbide (SiC), cordierite ($2MgO\text{-}2Al_2O_3\text{-}5SiO_2$), or metallic structures that can provide the requisite properties (Reşitoğlu, 2016).

The filter walls were constructed with a specific level of optimal porosity, which permits the efficient passage of exhaust gases across the walls while simultaneously ensuring the requisite impermeability to collect the diverse range of particulate species. The soot coating of the filter with soot results in the formation of a layer of soot on the surface of the duct walls. This guarantees the subsequent working phase will proceed with optimal efficiency through the utilization of surface filtration. It is of the highest importance to avoid the application of excessive quantities of soot. As the filters accumulate particulate matter (PM), a phenomenon known as back pressure is created. This can result in increased fuel consumption, engine failure and stress on the filter. To prevent these adverse effects, the diesel particulate filter (DPF) must undergo a process of regeneration, whereby the accumulated particulate matter (PM) is burned. This can be accomplished through two principal methods: active and passive regeneration. In the case of active regeneration, the soot that has been adsorbed is removed through a controlled oxidation process with oxygen at temperatures exceeding 550 °C (Jeguirim et al., 2005).

2.3.3. Lean NO_x Trap (LNT)

The Lean NO_x Trap represents one of the methodologies employed to curtail NO_x emissions. It is also referred to as the NO_x Storage Catalyst, NO_x adsorber catalyst, and NO_x Storage Reduction. In the event that the engine is operating in a fuel-lean condition, the Lean NO_x Trap will adsorb the NO_x; conversely, when the engine is operating in a fuel-rich environment, the stored NOx will be released into the exhaust gases (Reşitoğlu, et al., 2015).

In the Lean NO_x Trap, platinum (Pt) is employed as an oxidation catalyst, while rhodium (Rh) serves as a reduction catalyst. Additionally, barium (Ba) and other oxides facilitate the storage of NO_x. NO_x reacts with oxidation catalyst and stored in LNT by the following reaction: (Çalışkan, 2021).

$$BaCO_3 + 2NO_2 + ½\ O_2 \leftrightarrow Ba\ (NO_3)_2 + CO_2$$

$$Ba\ (NO_3)_2 + 3CO \rightarrow BaCO_3 + 2NO + 2CO_2$$

$$2NO + 2CO \rightarrow N_2 + 2CO_2$$

2.3.4. Selective Catalytic Reduction (SCR)

The most prevalent method employed in the reduction of nitrous oxide (NO_x) emissions from vehicle exhausts entails the utilization of both catalysts and reductants. This approach, known as selective catalytic reduction, has become a dominant technology in this field. This emission control technology is a system that has been developed specifically for heavy-duty vehicles. Due to the relatively low exhaust temperature of light-duty vehicles, the rate of utilization of this technology in such vehicles is less than that observed in heavy-duty vehicles.

SCR exhaust aftertreatment system enables the transformation of nitrogen oxide (NO_x) emissions, which are a consequence of diesel combustion, into water (H_2O) and nitrogen (N_2). The transformations are carried out with the assistance of the catalyst and reductant present within the system. In the literature, numerous researchers have sought to enhance this system by modifying the catalyst and reductant structures. Additionally, a considerable body of research has been conducted on the utilization of diverse reductants and multi-metallic catalysts to assess the catalytic performance of the SCR system (Özarslan, 2022).

A catalytic conversion process is employed to transform NO_x present within the exhaust gas into other substances, including water and N_2 gases. In view of the deleterious effects of NH_3, and with a view to preventing the combustion of NH_3 in the warm atmosphere prior to the reaction, NH_3 is provided from an aqueous solution of urea (Keskin et al., 2016).

Ammonia (Urea) SCR (NH_3 – SCR)

Selective catalytic reduction of nitric oxide with ammonia (NH_3-SCR) is represents an efficacious technological solution to the issue of nitric oxide emissions. Despite significant advancements in the development of NH_3-SCR catalysts over the past few decades, there remain significant hurdles in meeting the increasingly stringent emissions standards. It is observed that the catalysts are exposed to conditions of considerable temperature and humidity throughout the course of the regeneration of the DPF, which may result in the phenomenon of hydrothermal ageing (Shan et al., 2020; Özarslan, 2022).

The catalyst represents a fundamental component of the SCR technology. The NH_3-SCR catalyst is typically situated in a downstream position relative to the DOC. The technology utilizing vanadium-titanium SCR catalysts has reached a satisfactory level of maturity. The catalysts have reached a sufficient level of maturity to become commercially viable and have subsequently been adopted on a wide scale in the power sector with the aim of mitigating atmospheric soiling. Molecular sieve refers to a material with a silico-alumina content and a pore structure characterized by regularity. Commonly used molecular sieve materials include ZSM-5, MFI, and others. The mineral zeolite is characterized by its microporous structure, comprising aluminosilicate units, and by its distinctive electronic properties, which result from its particular molecular sieve structure. In order to enhance the functionality of the active phase, it is possible to modify it through ion exchange at the surface (Zang et al., 2024).

In the present era, zeolite catalysts are employed extensively due to their capacity to function across a broader range of application temperatures. This includes, copper-exchanged zeolites and iron-exchanged zeolites, which demonstrate superior performance at low and high temperatures, accordingly, have emerged as the primary means of regulating low NO_x emissions in vehicles. The power dynamics modelling of NH_3-SCR has been the subject of extensive research by numerous experts in the field with the objective of developing highly reliable SCR technology that complies with current and future NO_x regulations. In the context of Cu-based catalysts, copper is typically understood as an active metal, supported on a carrier. In this configuration, copper has a metallic oxidation state. In the formation of a molecular sieve, it typically exists in the ionic state (Zang et al., 2024).

It is crucial to examine the impact of concurrent NO_2 presence in diesel exhaust, as it may contribute to NO_x reduction via two distinct pathways. Two options are available for consideration: the "fast SCR" reaction and the conventional SCR reaction (Shan et al., 2020).

Fast SCR: $2NH_3 + NO + NO_2 \rightarrow 2N_2 + 3H_2O$

Standard SCR: $4NH_3 + 4NO + O_2 \rightarrow 4N_2 + 6H_2O$

Carbon monoxide SCR (CO – SCR)

Carbon monoxide (CO) emissions represent a significant environmental and human health concern. In light of the current deterioration in the environmental protection situation, there is a growing awareness among the general public of the need to protect themselves. This makes it essential to reduce NO_x and CO emissions. In order to reduce these two pollutants, the most common catalytic method is CO oxidation and CO selective reduction (CO-SCR). Today, a number of precious metal catalysts have become highly sought after due to their exceptional catalytic activity in CO-SCR and CO oxidation (He et al., 2022).

CO has been demonstrated to be one of the most effective reductants for the removal of NO_x due to its presence in exhaust emissions from vehicles and its relatively straightforward production by engine control. Despite this, carbon monoxide (CO) was previously considered an unsuitable reductant for selective catalytic reduction (SCR). This was due to the rapid consumption of CO by the reaction with oxygen (O_2) when supported by noble metal catalysts (Hamada and Haneda, 2012).

It is imperative to identify an economical catalyst material that can effectively substitute the noble metal catalyst in CO-SCR and CO oxidation processes. The unique properties of transition and rare earth metals, including their inherent valence and exceptional oxidative capabilities, have made them highly attractive for use in environmental catalysis. Ce-based catalysts are preferred due to their improved redox capacity, superior oxygen mobility and high oxygen storage capacity. However, the activity of pure cerium oxide and poor thermal stability limit their use (He et al., 2022).

The general reactions to CO-SCR are represented by: (Özarslan, 2022).

$$NO + CO \rightarrow 1/2N_2 + CO_2$$

$$NO_2 + 2CO \rightarrow 1/2N_2 + 2CO_2$$

$$2NO + 2CO \rightarrow N_2 + 2CO_2$$

Hydrogen SCR (H_2 - SCR)

In the case of rich oxygen cases, the efficiency of NH_3-SCR in reducing NO emissions has resulted in a relative lack of interest in H_2-SCR. Notwithstanding the aforementioned evidence, numerous studies have demonstrated that H_2-SCR can serve as an effective reductant under lean conditions. The majority of these studies have utilized platinum group metals as the active component, suggesting that this is a viable approach for achieving the desired outcome (Hamada and Haneda, 2012).

H_2-SCR offers numerous advantages. To illustrate, the use of hydrogen as a reductant does not result in the generation of secondary pollutants and exhibits high activity for the efficient reduction of NO_x at relatively low temperatures. As hydrogen (H_2) is a highly accessible resource for

industrial sites, the utilization of H_2-SCR is regarded as a prospective alternative to ammonia (NH_3)-SCR. It can be reasonably argued that the catalyst represents the technology that is the most essential to any H_2-SCR process, and its performance directly affects the amount of nitrogen oxides that can be removed. Noble metals are scarce and costly, and they are susceptible to sulfur poisoning. Their extensive utilization is restricted due to above reasons. Consequently, novel highly efficient catalysts must be identified to supplant Pt- and Pd-based catalysts for H_2-SCR for NO_x. Transition metal oxides are used extensively as catalysts in a number of different reactions due to a number of factors, including their cost-effectiveness, ease of synthesis and favourable redox properties (Cai et al., 2016).

Hydrocarbon SCR (HC - SCR)

The most practical approach is to replace ammonia or urea with hydrocarbons, a process known as hydrocarbon selective catalytic reduction (HC-SCR). Hydrocarbon Selective Catalytic Reduction (HC-SCR) is a promising approach for the removal of nitrogen oxides (NO_x). To enhance the chemical reactions of NO_x-SCR by hydrocarbons, a detailed understanding of the HC-SCR process at the molecular level is essential (Sawatmongkhon, 2011).

One of the crucial elements that must be considered in this system is the type of reductant. The NO_x conversion performance of the system is dependent on the type of reductant used. There are several options available for reductant selection in the system, including oxygenated hydrocarbons, hydrocarbons with varying carbon content, diesel fuel, and alcohols. Researchers have investigated the use of HC reductants at low temperatures as a potential strategy to enhance NO_x conversion efficiency (Özarslan, 2022).

3. PRELIMINARY WORK

In this chapter, it is analyzed the previous studies about scope of NO_X reduction with selective catalytic reduction.

As has been reported by numerous researchers, one of the key advantages of SCR over the NO_x storage catalyst is that it is highly effective when utilizing different reductants, which include urea, oxygenated hydrocarbons and hydrocarbons. Similarly, SCR has been demonstrated to be effective with a range of catalyst materials, including ion-exchanged zeolites, copper, platinum and silver, while the choice of catalyst support, for example Al_2O_3, SiO_2, ZrO_2 and TiO_2, has also been shown to affect the effectiveness of the process (Sawatmongkhon, 2011).

He et al. used Zirconium phosphate supported copper catalyst in their studies. The comprehensive characterization through X-ray diffraction (XRD), scanning electron microscopy (SEM), and transmission electron microscopy (TEM) revealed that the copper (II) species were extensively dispersed on α-zirconium phosphate and could be bonded with the phosphate group of the support (He et al., 2023)

He et al. studied on Cu-doped Ce-based mixed metal oxide catalysts. Among the tested catalytic materials, the $10Cu/CeO_2$ catalyst demonstrated the highest level of activity and stability in both reaction types. The catalysts were subjected to a series of characterization techniques, including XRD, BET, SEM, TEM, XPS, H_2-TPR, Raman, O_2-TPD, and in-situ DRIFTS. The data demonstrate that the selective orientation of CeO_2 crystallographic planes is conducive to the dispersal of Cu species. Additionally, the incorporation of Cu into Ce-based catalysts expands the spectrum of active oxygen species present on the catalyst surface, enhances the mobility of oxygen, and, as a consequence, elevates the catalyst's activity (He et al., 2022).

Wang et al. produced ruthenium catalyst incorporated zirconium phosphate. The present study demonstrates that zirconium phosphate (ZrP) is a valuable inorganic material with noteworthy characteristics, including high thermal stability and high water tolerance (Wang et al., 2016).

According to studies of Pan et al., they investigated catalytic reduction of NO by CO with Cu-based and Mn-based catalysts. Catalytic performance tests indicate that the $Cu\text{-}Ce\text{-}Fe\text{-}Co/TiO_2$ and $Mn\text{-}Ce\text{-}Fe\text{-}Co/TiO_2$ catalysts display the highest catalytic activity for the reduction of NO with CO, when compared to other Cu-based and Mn-based catalysts, respectively. In comparison to the $MnCe\text{-}Fe\text{-}Co/TiO_2$ catalyst, the $Cu\text{-}Ce\text{-}Fe\text{-}Co/TiO_2$ catalyst exhibits greater tolerance to the presence of O_2, SO_2 and H_2O(g) (Pan et al., 2020).

In a comparative study of $Cu\text{-}Al_2O_3$ and Ag/Al_2O_3 catalysts for C_3H_6-SCR of NO_x, He et al. observed that Ag/Al_2O_3 exhibited enhanced activity for NO_x reduction, while $Cu\text{-}Al_2O_3$ demonstrated superior activity for C_3H_6 oxidation under unfavorable conditions (He et al., 2004).

4. MATERIAL AND METHOD

This chapter is divided into three sections. The first section identifies the materials and chemicals used in preparing the catalyst and in the coating process. The second section provides a detailed explanation of the steps involved in the coating process. The third section presents technical information about the devices used in catalyst preparation and analysis, as well as about the chemical and structural properties of the catalyst. Finally, the chapter provides information about the emission test system, which is used to test the catalyst under real conditions. It also provides information about the technical features of the equipment in the system and about the programs used during the test.

4.1. Properties of Materials Used in Catalyst Preparation and Performance Tests

4.1.1. Properties of Cordierite

In this study, ceramic a monolith honeycomb cordierite ($2Al_2O_3$- $5SiO_2$-2MgO) cordierite with a cell density of 400 cpsi (cells per square inch) and a length of 100 mm, a diameter of 130 mm was employed as the carrier material. Cordierite was selected as the experimental carrier material due to its advantageous properties, including high catalytic loading capacity, durability, material strength, low coefficient of thermal expansion, and low cost, when compared to other carrier structures (Çalışkan, 2021; Özarslan, 2022).

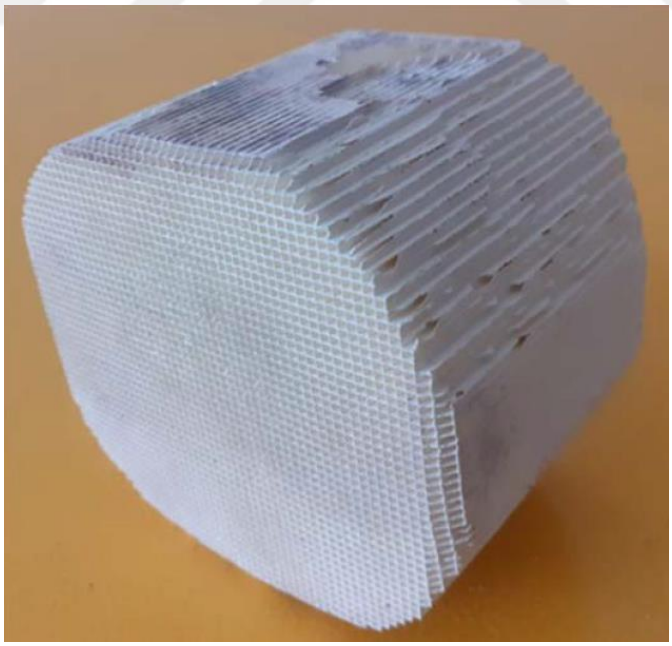

Figure 4.1. Monolith Honeycomb Cordierite

Figure 4.2. Catalyst after test process

4.1.2. Oxalic Acid Dihydrate ($C_2H_2O_4$ *$2H_2O$)

Oxalic acid was used during preparing the catalyst to increase the surface area of cordierite. The used oxalic acid was Supelco branded. Chemical formula of Oxalic Acid is $C_2H_2O_4$*$2H_2O$ and also the CAS number is 6153-56-6. Molar mass of $C_2H_2O_4$ is 126,07 g/mol. Oxalic acid has 149-160 °C boiling point at 1013 hPa, 1.65 g/cm3 density at 20 °C and 98-100 °C melting point.

4.1.3. Zirconium Dioxide (ZrO_2)

In contrast to other ceramic materials, zirconium oxide (ZrO_2), also known as zirconia, exhibits an exceptionally high resistance to crack propagation. Additionally, zirconium oxide ceramics exhibit high thermal expansion, rendering them a frequently utilized material for joining ceramic and steel components (CeramTec, Low Thermal Conductivity meets High Strength).

Zirconium phosphate (ZrP) has been identified as a valuable inorganic material, exhibiting notable characteristics such as high thermal stability and high-water tolerance (Wang et al., 2016).

Aldrich brand Zirconium (IV) oxide material was used in this study.

4.1.4. Copper (II) nitrate trihydrate ($Cu(NO_3)_2 \cdot 3H_2O$)

Copper (II) Nitrate Trihydrate was used for catalyst preparation in this study. The used copper (II) nitrate trihydrate was Carlo Erba Reagents branded. Chemical formula of Copper (II) Nitrate Trihydrate is Cu $(NO_3)2x3H_2O$ and also the CAS number is 10031-43-3 and the EC number is 221-838-5. Density of Cu $(NO_3)_2x3H_2O$ at 20 0 C is 2.05 g/cm^3. Copper (II) Nitrate Trihydrate has 114 ^{0} C melting point.

4.1.5. Ammonium dihydrogen phosphate $(NH_4)H_2PO_4$

The superior coordination and accelerate electron transport capabilities of phosphate were leveraged to synthesize a catalyst with different ratios of P using eco-friendly ammonium dihydrogen phosphate (ADP) (Zang et al., 2024). Supelco brand ADP was used as material.

4.1.6. Ethanol (CH_3CH_2OH)

Alcohol varieties are employed as reductant agents in scientific investigations pertaining to the performance of selective catalytic reduction (SCR) systems. In this study, ethyl alcohol was employed as a reductant agent in the formation of mixtures. The chemical formula of ethyl alcohol is C_2H_5OH, and its CAS number is 64-17-5. The molar mass of C_2H_5OH is 46.07 g/mol, and the compound has a purity of ≥ 99.9%. The boiling point of ethyl alcohol is 78.3°C at 1013 hPa, the density is 0.790–0.793 g/cm³ at 20°C, and the melting point is -114.5°C (Özarslan, 2022).

4.2. Technical Properties of The Devices Used in Catalyst Preparation

This chapter outlines the properties and technical specifications of the devices utilized in catalyst preparation.

4.2.1. RADWAG AS 220.R2

Technical properties of RADWAG AS 220.R2 shown in Table 4.1. and picture given in Figure 4.3.

Table 4.1. Technical properties of RADWAG AS 220.R2

Maximum Capacity	220 g
Minimum Capacity	10 mg
Precision	0.1 mg
Repeatability	0.1 mg
Operating Temperature	+10 °C - +40 °C
Power Supply	12 / 16 V DC
Response Time	3.5 s
Calibration Type	Automatic
Net Weight	5.6 kg

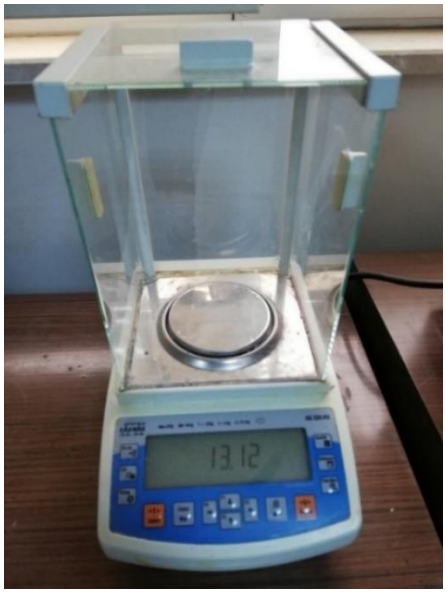

Figure 4.3. RADWAG AS 220.R2

4.2.2. Drying Oven

During the catalyst preparation drying process, the MEMMERT BAIC UNB 500 oven was employed for the purpose of drying. MEMMERT BAIC UNB 500 Oven are provided in the Figure 4.4.

Figure 4.4. MEMMERT BAIC UNB 500 Oven

4.2.3. Sintering Oven

During the catalyst preparation process, sintering was conducted using a Protherm Model PLF 110/6 Oven. The table 4.2. shows the technical properties of the aforementioned oven.

Table 4.2. Protherm Model PLF 110/6 Oven

Model	PLF 110/6
Maximum Temperature	1100 °C
Maximum Operating Temperature	1050 °C
Time to Reach Maximum Temperature	45 min
Volume	6.3 liters
Inner Dimensions	15*21*20cm
Outer Dimensions	65*55*58 cm
Maximum Power	2 kW
Voltage	220 V
Phase	1

Figure 4.5. Protherm Model PLF 110/6 Oven

4.2.4. Magnetic Stirrer

In the production of the catalysts, magnetic stirrers of the MTOPS MS300 HS brand and model were employed for the preparation of the solution. (Figure 4.6.)

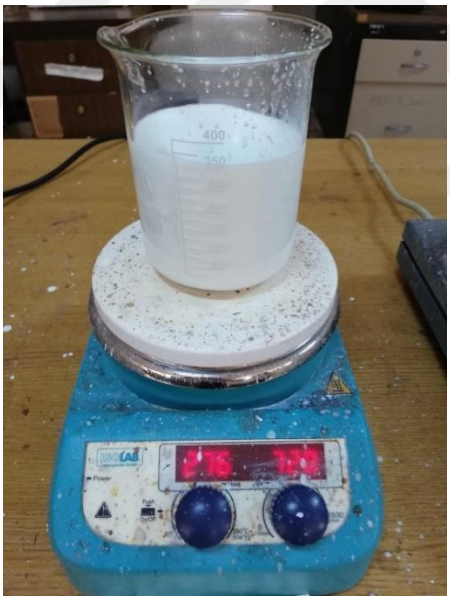
Figure 4.6. Magnetic Stirrer

4.3. Acid Treatment and Characterization of Cordierite

The study employed ceramic cordierite with a cell density of 400 cpsi (cells per square inch) and a length of 100 mm, a diameter of 130 mm. Cordierite test specimens were extracted from the blank cordierite material and machined to the same dimensions as illustrated in Figure 4.7. These structures were subjected to a series of treatments at varying durations and oxalic acid ($C_2H_2O_4*2H_2O$) ratios with the objective of enhancing the specific surface area at the initial stage of catalyst production.

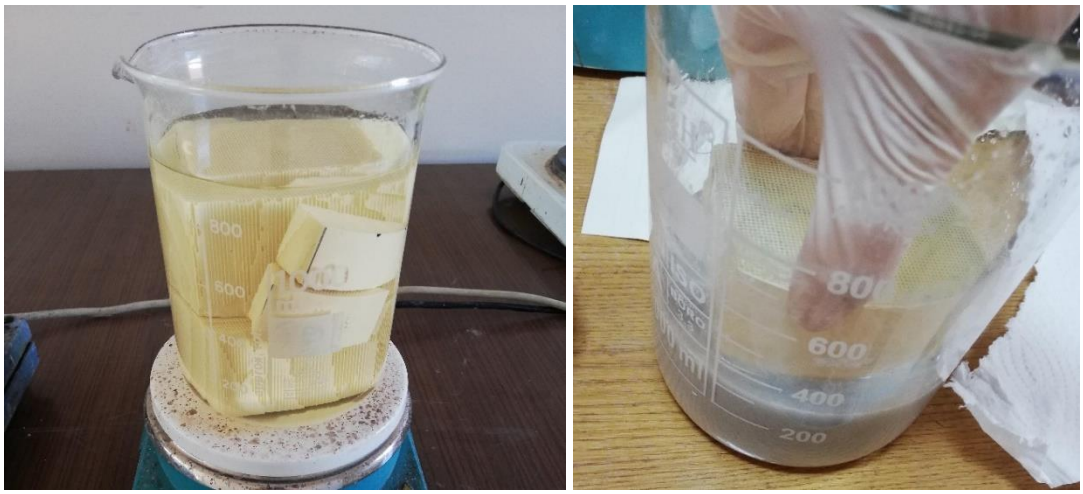

Figure 4.7. Acid treatment process for catalyst samples

4.4. Catalyst Preparation

In the production of the catalyst, cordierite ($2Al_2O_3 – 5SiO_2 – 2MgO$) with 400 cpsi square pores and a one-piece monolithic host structure were used. Prior to coating, the cordierite material was subjected to a pretreatment process involving the use of a mixture of 250 grams of oxalic acid and 500 ml of pure water for each sample. This was done to enhance the surface area of the surface to be coated. This pretreatment was applied at 90 ℃ for 4 hours. The aforementioned pretreatment was completed, and the cordierite material was prepared for the coating process. In order to prepare the mixture, 5.72 grams ($(NH_4)H_2PO_4$) and 4.973 grams ($Cu\ (NO_3)_2 3H_2O$) were used. The mixture was mixed with 300 ml of pure water. The mixture was then stirred for one hour with the assistance of an ultrasonic mixer. Subsequently, SiO_2 was incorporated into the mixture at a rate of 1 wt% of the powder catalyst, with the objective of enhancing the binding properties. The mixture was stirred at 90 ℃ with the help of an ultrasonic mixer until the water evaporated. Then the mixture was baked at 110 ℃ for 1 hour to completely evaporate the water in the mixture. The mixture was subsequently subjected to calcination at 550 °C for a period of two hours. A quantity of 40 grams of the powdered mixture, comprising particles of P, Cu, and Zr, was taken and the mixture was prepared once more with 400 milliliters of pure water. The cordierite material was immersed in the mixture 3 times for each catalyst, thereby initiating the coating process. Subsequently, the cordierite material was subjected to a drying process in an oven at 120 °C for one hour, followed by calcination at 550 °C for three hours. Upon completion of these processes, the catalyst was produced. Specifications of produced catalysts were given in table 4.3.

Table 4.3. Materials of Prepared Catalysts

Catalysts Number	Catalyst material ratios		
	P	**Cu**	**ZrO_2**
Catalyst I	4 wt. %	-	96 wt. %
Catalyst II	3 wt. %	1 wt. %	96 wt. %
Catalyst III	2 wt. %	2 wt. %	96 wt. %
Catalyst IV	1 wt. %	3 wt. %	96 wt. %
Catalyst V	-	4 wt. %	96 wt. %

4.5. Catalyst Characterization Equipment and Technical Properties

This chapter presents the technical details of the instrumentation employed for the analysis of the catalysts, including X-ray diffraction (XRD), Brunauer-Emmett-Teller (BET) analysis, and scanning electron microscopy (SEM).

4.5.1. X – Ray Diffraction (XRD)

X-ray diffraction (XRD) is predicated on the principle that each crystalline phase refracts X-rays in a distinctive manner, contingent on their distinctive atomic sequences. The X-ray diffraction apparatus enables the qualitative and quantitative investigation of crystal materials and thin films.

4.5.2. BET Analysis

The BET analysis device is capable of detecting surface area measurements, micro, meso, and macro pore measurements, and pore size distribution at low pressures and with high resolution in solid or powder samples by the physical adsorption method. The device employs the Brunauer, Emmet, and Teller (BET) method, which is used to measure surface area and porosity based on the nitrogen (N_2) gas adsorption technique in a liquid nitrogen environment at 77 °K.

4.5.3. SEM Analysis

Scanning electron microscopy (SEM) is a test that employs an electron beam to scan a sample, thereby producing a magnified image. A scanning electron microscope (SEM) is capable of conducting analyses on a variety of solid specimens, including metals, textiles, fibers, and plastic polymers. Additionally, samples that are not conductive can be coated with a thin layer of conductive material, approximately 2Å/second in thickness, and subsequently analyzed. Electron microscopy is conducted at high magnifications, generates high-resolution images, and precisely measures very small features and objects. The data obtained from SEM analysis provides information regarding the specimen's morphology (texture), crystalline structure, the orientation of the materials present in the sample, and chemical composition.

4.6. Test System for The Measurement of NO_x Emissions

In this section, the components employed in the experimental test system are listed and a detailed explanation is provided for each.

4.6.1. Performance Test System Overview

Produced catalysts were tested in the setup which is illustrated in Figure 4.8.
An Aksa brand 2-cylinder diesel engine was conducted during tests. Ethanol was used as reductant.

Experiments were conducted at three different engine loads 0-2-4 Kw. A loading unit was employed due to obtain different engine loads. Tests were performed at the temperature between 170 and 240 °C with the constant space velocity (40000 h^{-1}).

Thus, NO_x conversion ratio was observed with the different parameters such as; material, temperature and engine load.

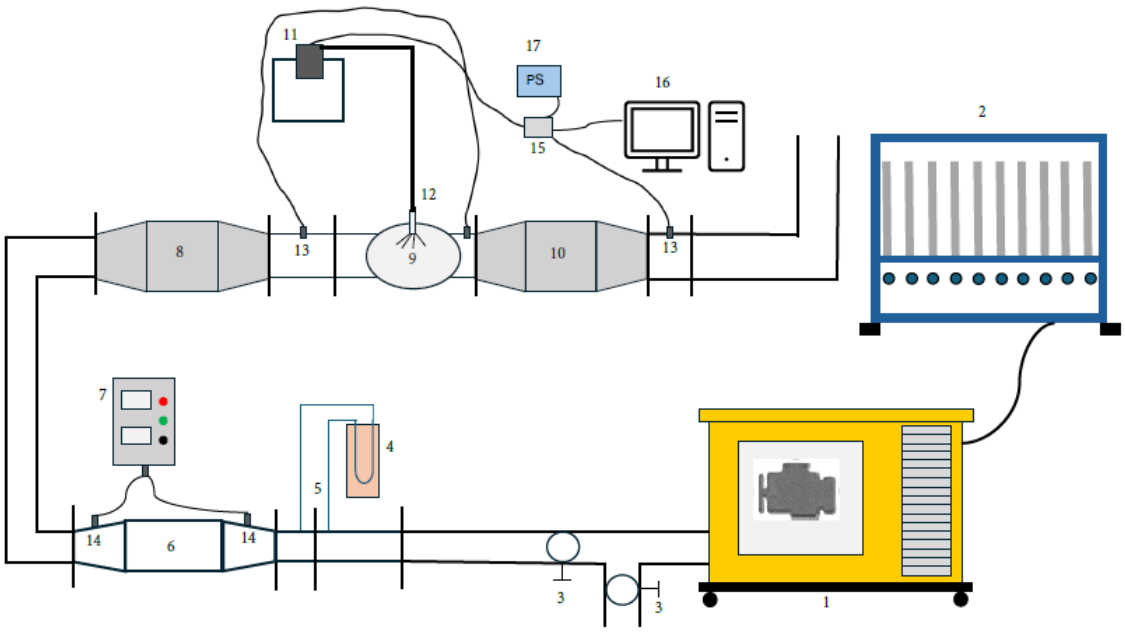

Figure 4.8. Experimental Setup

1- Diesel Test Engine
2- Electric Loading Unit
3- Valves
4- Manometer
5- Orifice Plate
6- Exhaust Gas Heating Unit
7- Heater Control Unit
8- DOC (Diesel Oxidation Catalyst)
9- Reductant injection chamber
10- SCR (Selective Catalytic Reduction)
11- Reductant Pump
12- Injector
13- NO_x Sensors
14- Thermocouples
15- SCR Control Unit
16- PC
17- 24V Power Supplier

4.6.2. Components Used in Test System

NO_x Sensor, Electronic Control System, test engine, Control Panel of The Exhaust Gas Heater, Electric Loading System, Orifice Plate and Manometer, Thermocouple, Control Panel of The Exhaust Gas Heater, Electric Loading System

Test Engine

In the laboratory experiments conducted to assess the NO_x conversion rate of the catalyst, a test engine manufactured by AKSA and designated as the A2CRX08 model was utilized. The test engine in question is equipped with a two-cylinder V-type diesel engine. The pertinent technical specifications pertaining to the AKSA brand A2CRX08 model test engine are presented in Figure 4.9. and technical specifications given in Table 4.3.

Table 4.4. Technical specifications of test engine

Motor Model	A2CRX08
Number of Cylinders	2
Motor Type	V-Type
Bore / Stroke	80 mm / 79 mm
Fuel Type	Diesel
Compression Ratio	23:1
Speed (rpm)	3000
Frequency (Hz)	50
Prime Power (kW)	9.6
Standby Power (kW)	8.8
Fuel Consumption (lt/hr)	4 lt/hr
Alternator Brand	Mecc Alte
Alternator Design	Brushed, 2 Poled
Electric System	12 V DC
Cooling Type	Water Cooled
Dimensions	1152 mm / 776 mm / 890 mm
Net Weight	270 kg

Figure 4.9. AKSA brand A2CRX08 model test engine

Control Panel of The Exhaust Gas Heater

The objective of this investigation was to ascertain the impact of temperature on catalyst performance. To this end, a series of experiments were conducted at temperatures spanning from 170 °C to 240 °C. The control panel plays a pivotal role in achieving the desired exhaust gas temperature.

Figure 4.10. Control Panel of The Exhaust Gas Heater

Electric Loading System

During the experiments, the test engine was loaded using a 10-kilowatt loading system, which is available in the Çukurova University Automotive Engineering Laboratory (as depicted in Figure 4.11. The NO_x emission rates were evaluated under varying load conditions, including 0 Kw, 2 Kw, and 4 Kw.

Figure 4.11. Electric Loading System

5. RESULTS AND DISCUSSIONS

This part demonstrates the characterization outcomes of the SEM, XRD, and BET analyses of the produced catalysts. The results of experiments demonstrated the impact of catalyst and ethanol reductant usage on NO_x conversion performance. The NO_x conversion efficiencies were discussed in the conclusion, and recommendations for future studies were presented. The table 5.1. gives the abbreviated names of the catalysts referred to in the experiments. The numerical and visual data obtained as a result of the analysis are given for each catalyst.

Table 5.1. Catalyst abbreviations

Catalyst	Catalyst abbreviations
$4P/ZrO_2$	4PZ
$3P-1Cu/ZrO_2$	3P1CZ
$2P-2Cu/ZrO_2$	2P2CZ
$1P-3Cu/ZrO_2$	1P3CZ
$4Cu/ZrO_2$	4CZ

5.1. Characterization Results of Acid-treated Cordierite

5.1.1. BET Surface Area Results

BET analysis was performed with the analysis absorptive N_2 and with 77.35 °K temperature. Table 5.2. shows the results of BET Surface area results for all catalysts. The catalysts utilized in the BET analysis have already been treated with oxalic acid and coated with the requisite materials. The BET surface area results illustrate a notable enhancement in surface porosity, which is a direct consequence of the oxalic acid treatment.

The BET surface area of the original cordierite material was about 0.5 m^2/g (Özarslan, 2022, Çalışkan, 2021). Previous studies have indicated that coating materials may affect surface area in either a decreasing or increasing manner, depending on the specific material properties involved (Keskin Z., 2019). According to results for BET surface area in Table 5.2.; surface area increased approximately 40 times for 4PZ, 28 times for 3P1CZ, 40 times for 2P2CZ, 36 times for 1P3CZ and 28 times for 4CZ catalysts. Comparing the results of 4PZ and 4CZ, it can be observed that phosphorus has a better contribution to the increase in surface area.

Table 5.2. BET analysis results of cordierite

Catalysts	BET Surface Area	Langmuir Surface Area	t-Plot Micropore Area	t-Plot External Surface Area
4PZ	20,1653 m^2/g	28,5796 m^2/g	3,4076 m^2/g	16,7577 m^2/g
3P1CZ	13,9181 m^2/g	19,6856 m^2/g	4,9921 m^2/g	8,9261 m^2/g
2P2CZ	19,1744 m^2/g	25,6769 m^2/g	11,1024 m^2/g	8,0721 m^2/g
1P3CZ	17,9325 m^2/g	25,3712 m^2/g	6,5850 m^2/g	11,3474 m^2/g
4CZ	13,6330 m^2/g	18,5413 m^2/g	7,1382 m^2/g	6,4948 m^2/g

5.1.2. SEM-EDS Analysis Results

The following series of visual representations provides an illustration of the surface morphology of the cordierite material, as observed through scanning electron microscopy and the catalyst produced following the coating process. The nano-sized surface structure of the cordierite material and the produced catalyst was investigated through the use of scanning electron microscopy (SEM) analysis.

The images captured during the SEM analysis were obtained at an accelerating voltage of 20 Kv and at two different magnifications, 5000x and 10000x. Below figures presents the SEM images of the cordierite material in nano dimensions, offering insight into its surface appearance. The images were captured at 5000x magnification and a 10 µm scale and 10000x magnification and a 5 µm scale.

As evidenced by the SEM images in Figure 5.1., 5.2., 5.3., 5.4. and 5.5., the cordierite material exhibits a porous structure. It is additionally notable that surface cracks were identified.

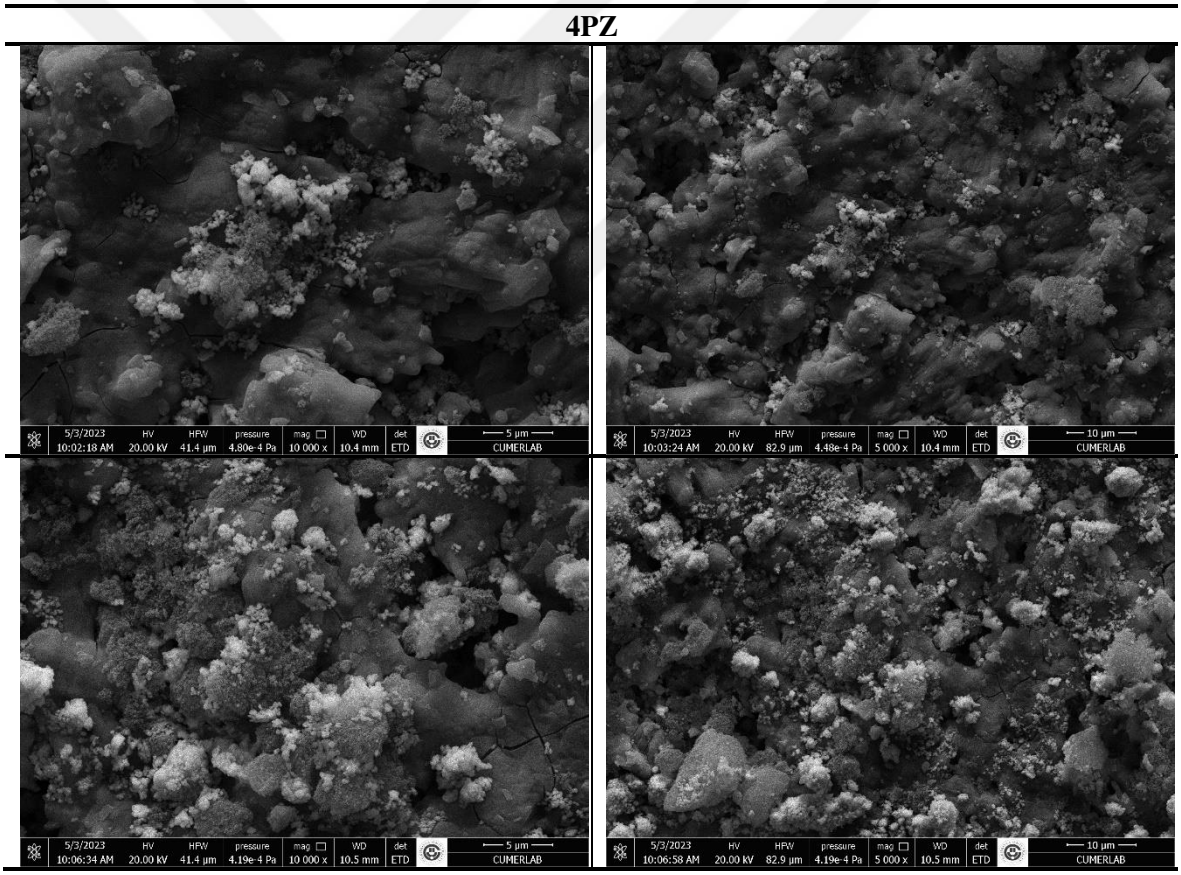

Figure 5.1. SEM images of Catalyst 4PZ

3P1CZ

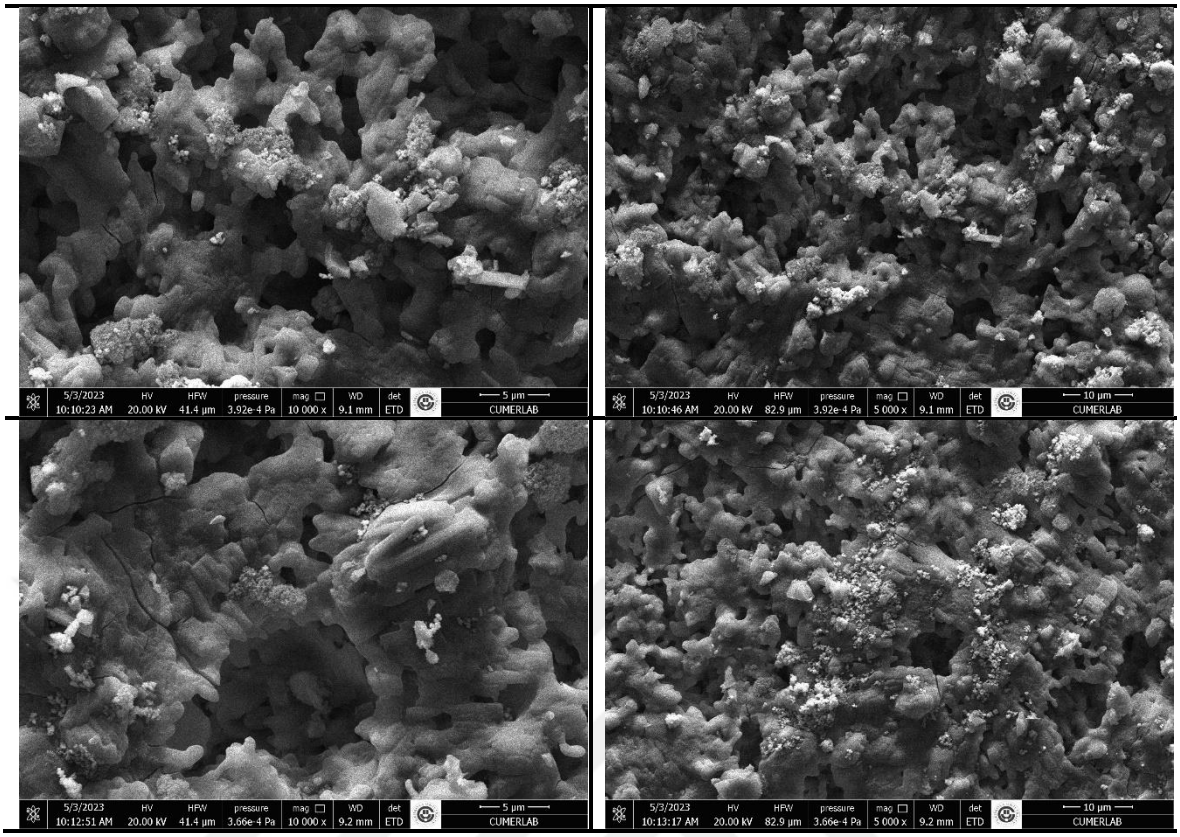

Figure 5.2. SEM images of Catalyst 3P1CZ

2P2CZ

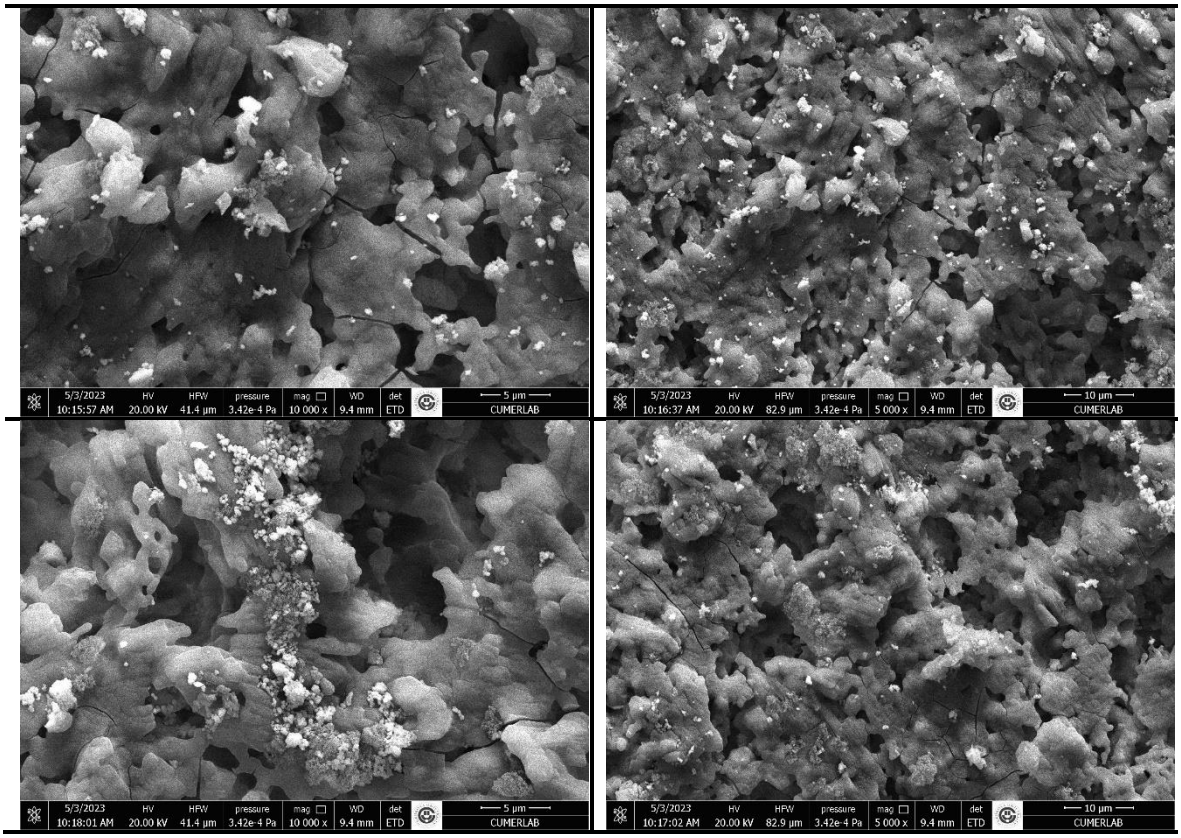

Figure 5.3. SEM images of Catalyst 2P2CZ

1P3CZ

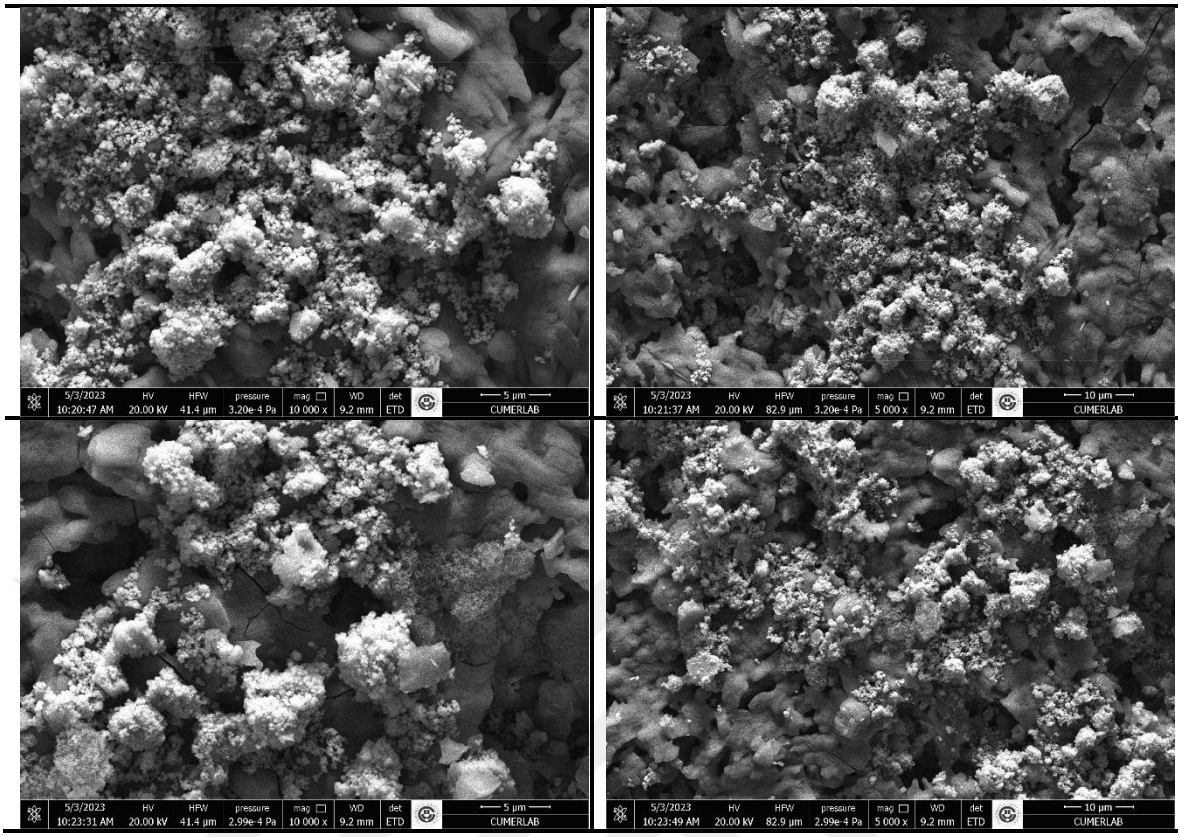

Figure 5.4. SEM images of Catalyst 1P3CZ

4CZ

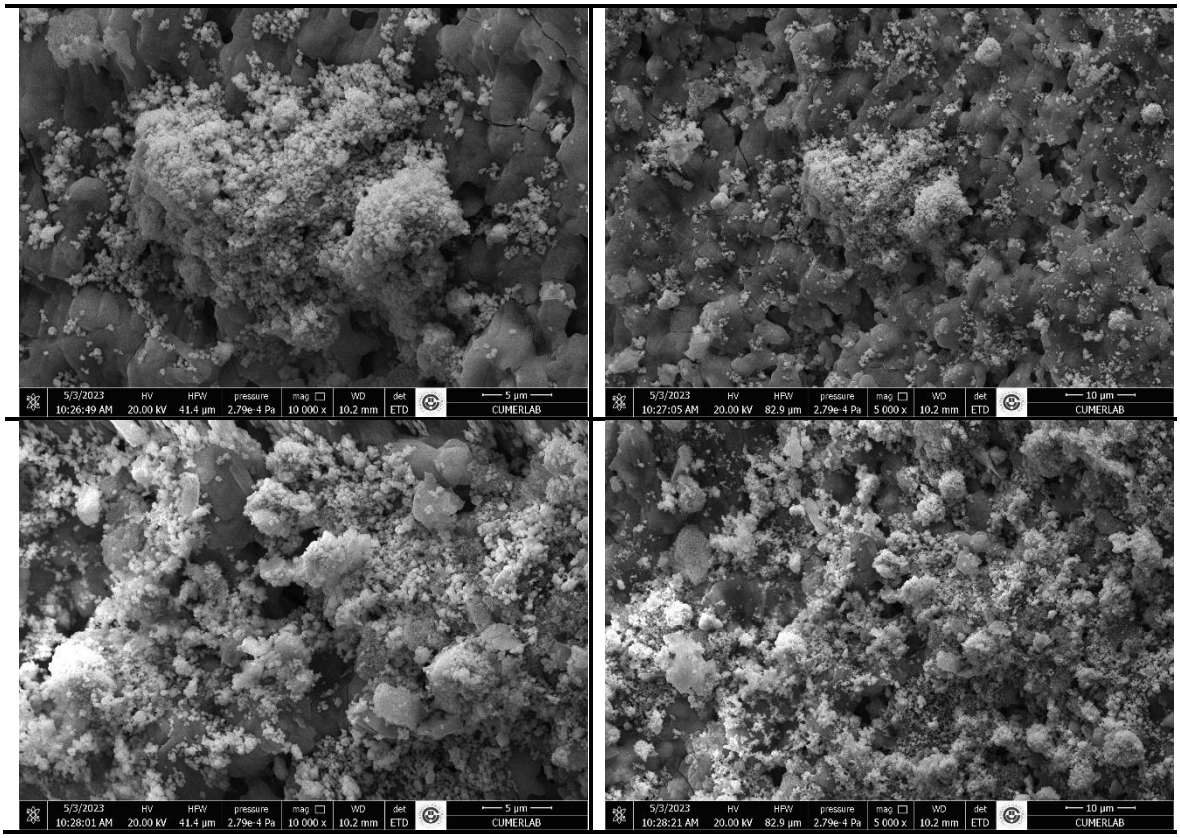

Figure 5.5. SEM images of Catalyst 4CZ

A complete scan of the catalyst's surface area was conducted using energy-dispersive X-ray spectroscopy (EDS). After coating, the presence of P, Cu, and Zr metal peaks on the cordierite structure was observed. The weight and atomic proportions of the components within the designated study region are presented in following figures.

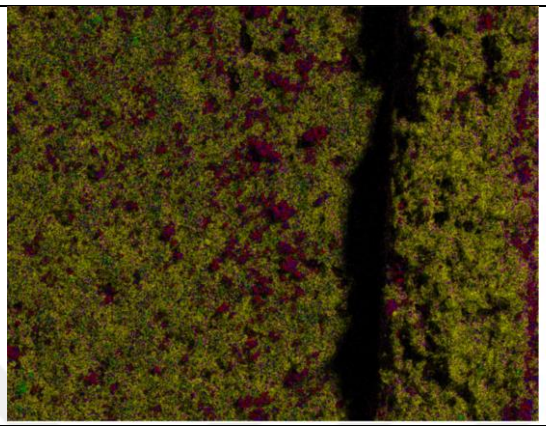

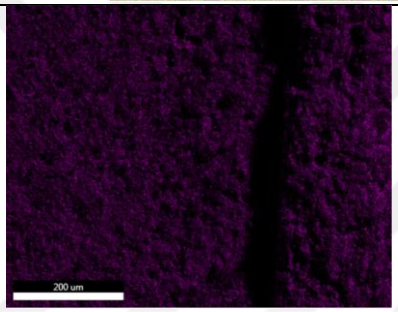

O K_ROI (23)

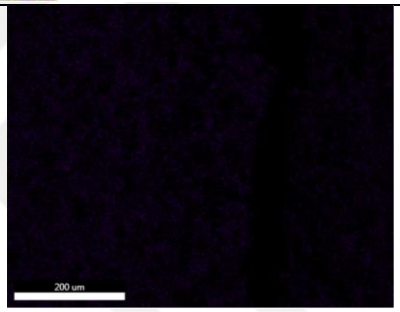

MgK_ROI (12)

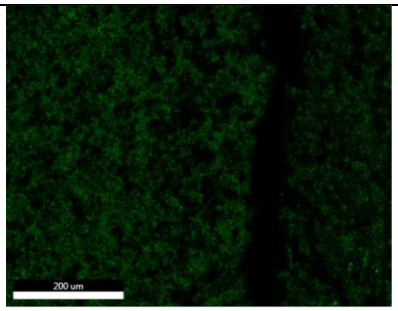

AlK_ROI (26)

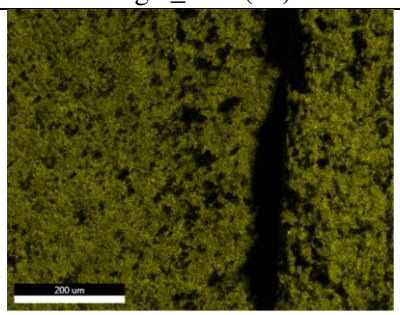

SiK_ROI (36)

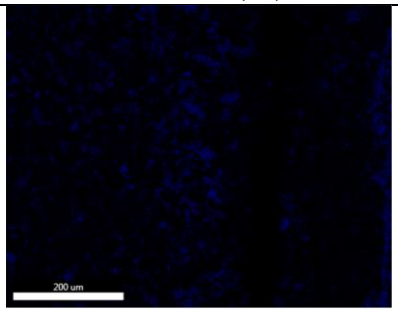

P K_ROI (19)

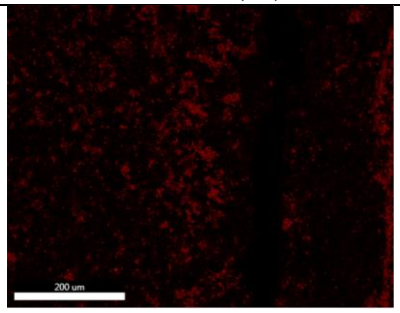

ZrL_ROI (28)

Figure 5.6. EDS Mapping Images of 4PZ Catalyst

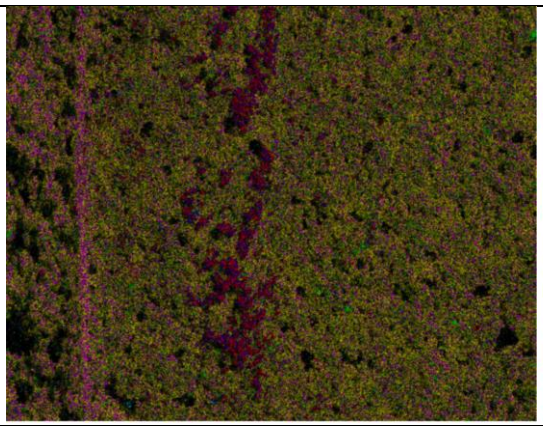

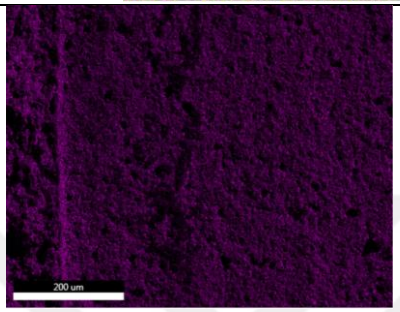

O K_ROI (22)

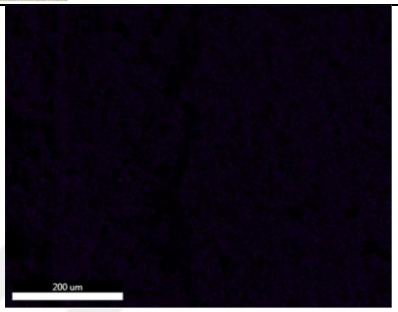

MgK_ROI (15)

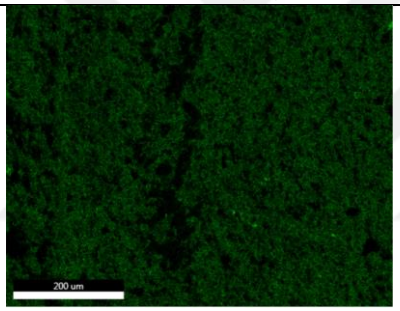

AlK_ROI (26)

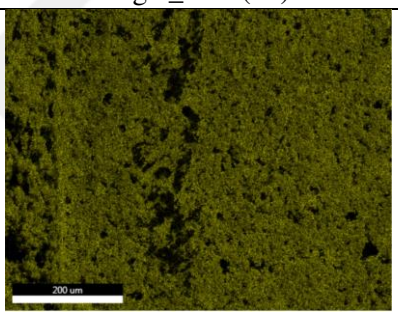

SiK_ROI (32)

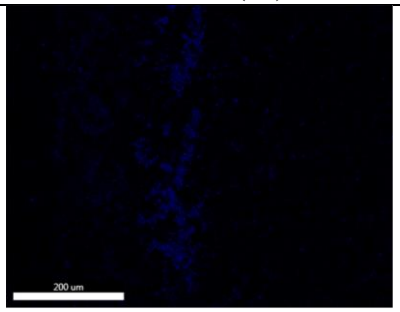

P K_ROI (16)

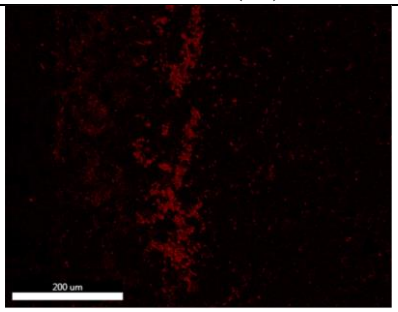

ZrL_ROI (24)

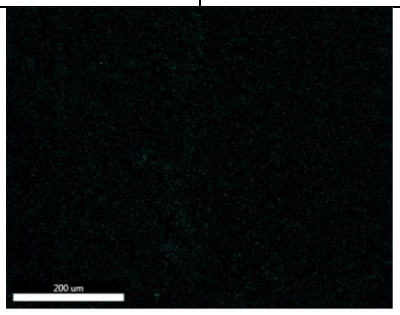

CuK_ROI (6)

Figure 5.7. EDS Mapping Images of 3P1CZ Catalyst

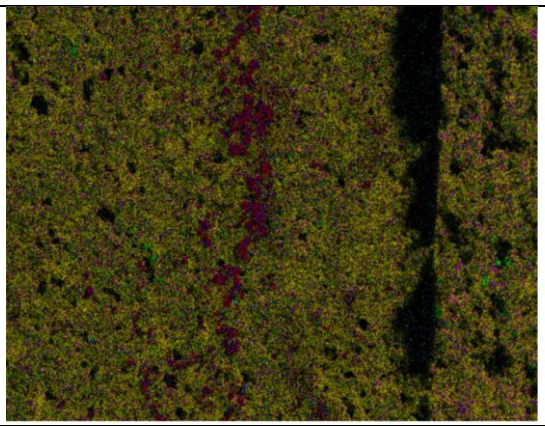

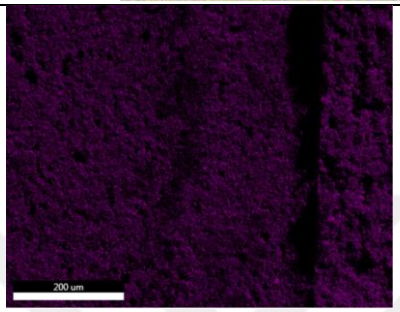

O K_ROI (22)

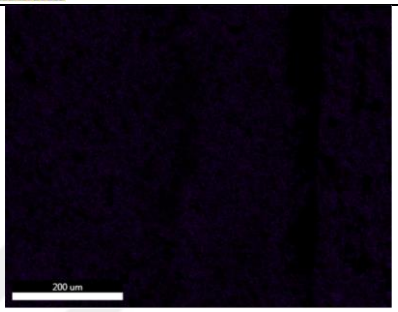

MgK_ROI (13)

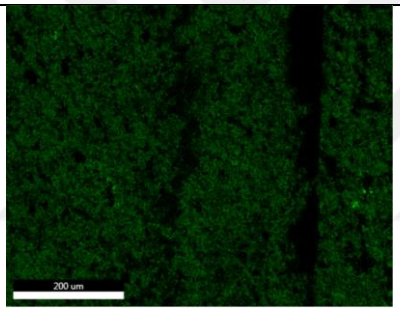

AlK_ROI (27)

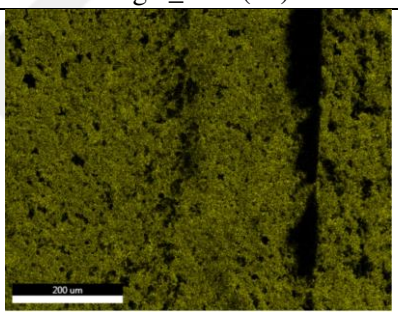

SiK_ROI (33)

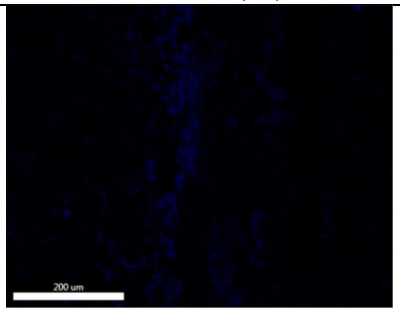

P K_ROI (18)

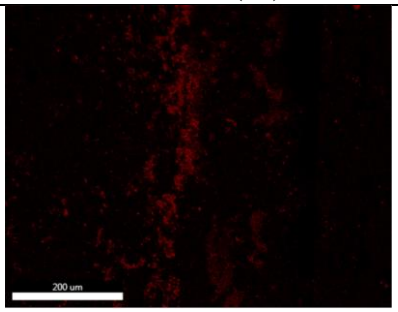

ZrL_ROI (27)

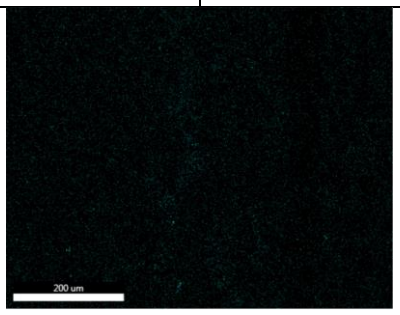

CuK_ROI (6)

Figure 5.8. EDS Mapping Images of 2P2CZ Catalyst

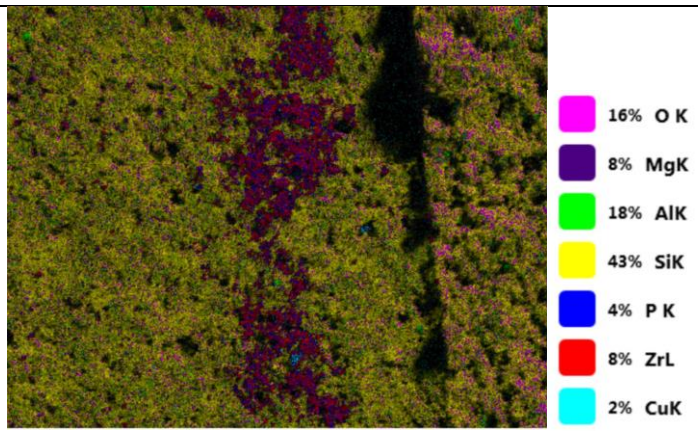

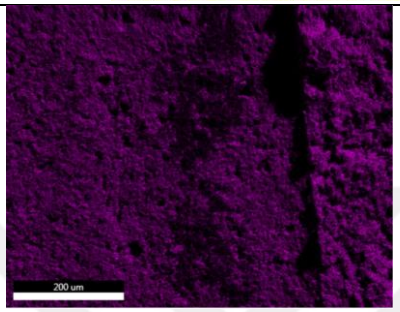

O K_ROI (34)

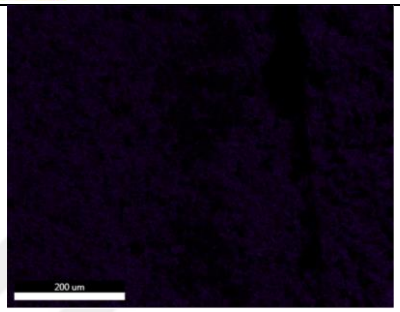

MgK_ROI (20)

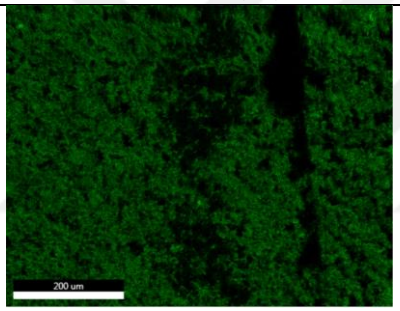

AlK_ROI (37)

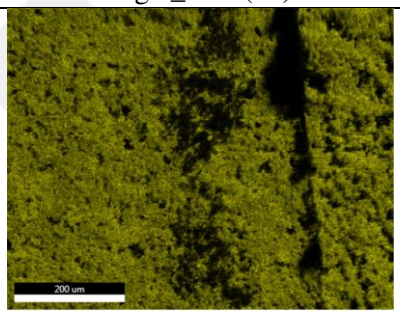

SiK_ROI (47)

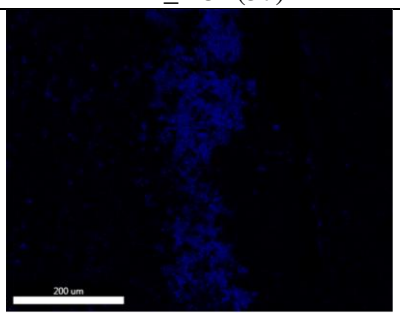

P K_ROI (18)

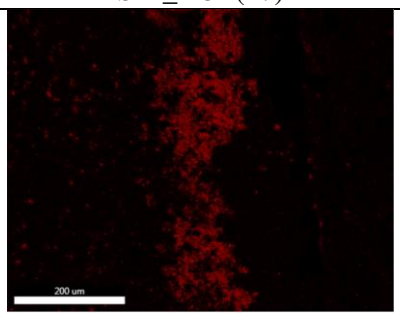

ZrL_ROI (27)

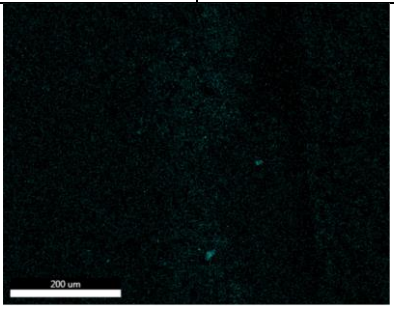

CuK_ROI (8)

Figure 5.9. EDS Mapping Images of 1P3CZ Catalyst

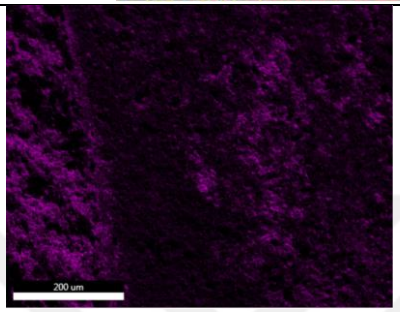

O K_ROI (36)

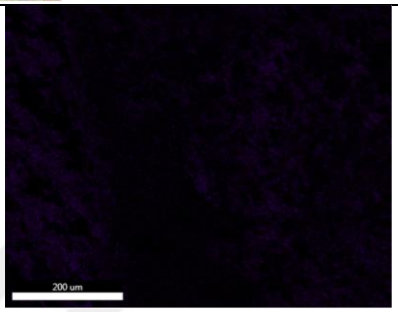

MgK_ROI (21)

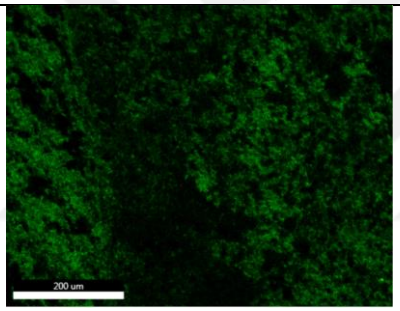

AlK_ROI (36)

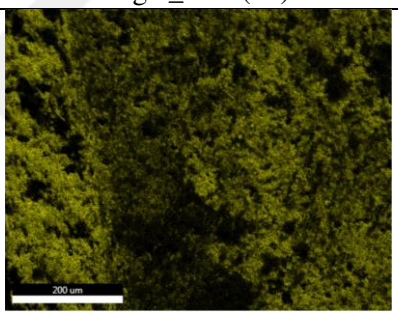

SiK_ROI (52)

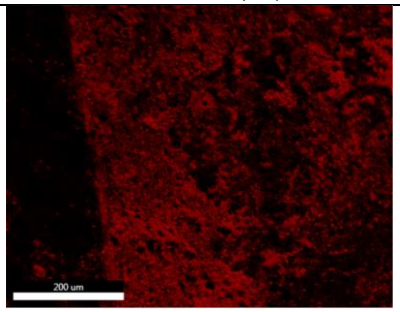

ZrL_ROI (59)

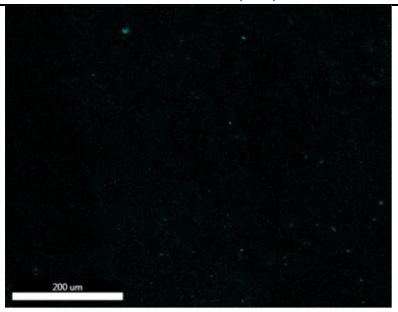

CuK_ROI (19)

Figure 5.10. EDS Mapping Images of 4CZ Catalyst

5.1.3. XRD Analysis Results

XRD analysis was performed to examine the crystal structure of materials. According to analysis results, peak values for each material obtained. Crystallographic parameters and material specifications are listed in following tables and figures for each sample.

Table 5.3. Formula and Crystallographic Parameters of 4PZ Catalyst

	Cordierite high	**O_2Zr_1**	**P_1**
Common name:	Cordierite high	Baddeleyite	Phosphorus
Chemical formula:	$Al_4Mg_2O_{18}Si_5$	O_2Zr_1	P_1
Crystal system:	Hexagonal	Monoclinic	Cubic

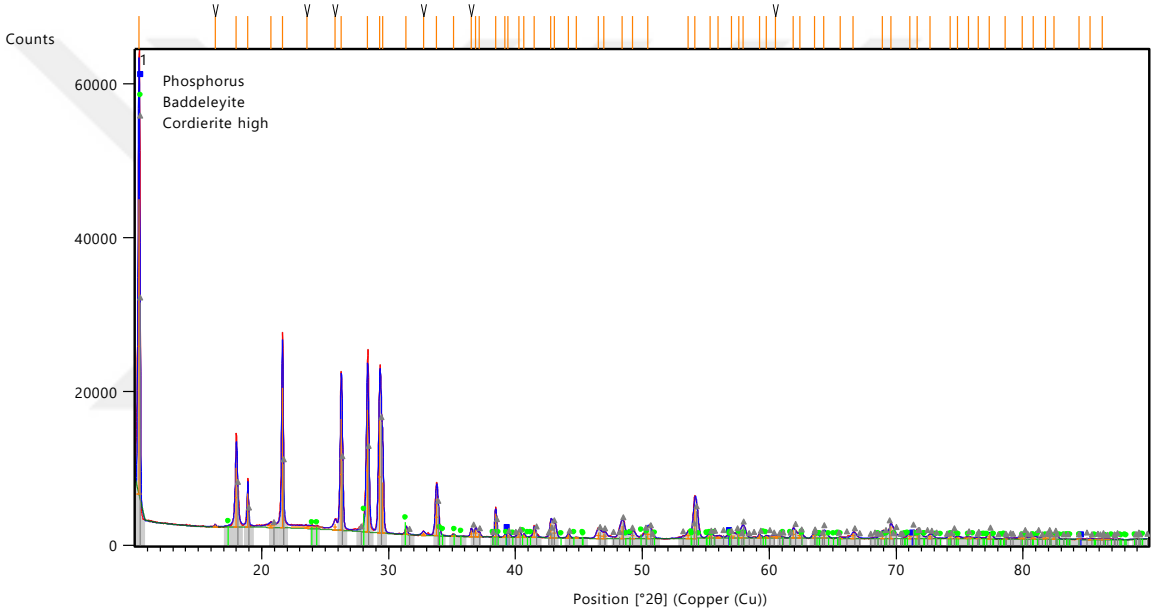

Figure 5.11. XRD analysis of 4PZ Catalyst

The XRD analysis for 4PZ catalyst shows that, the crystal structure of cordierite ($Al_4Mg_2O_{18}Si_5$) hexagonal. Other materials inside the catalyst are; Baddeleyite (O_2Zr_1) in monoclinic crystal system and Phosphorus (P_1) in cubic crystal system. (Table 5.3.)

Figure 5.11. demonstrate the peak values of Phosphorus, Baddeleyite and Cordierite high.

Peak points for Cordierite high; 2θ = 10.431º, 21.711º, 26.362º, 28.420º, 29.458º, 54.26 º. Peak points for Baddeleyite; 2θ = 24.349º, 28.05º, 31.333º, 33.985º, 34.25º, 35.152º, 40.541º, 49.893º, 50.316º, 53.838º. Peak points for Phosphorus; 2θ = 39.312º, 56.811º, 71.27º.

Table 5.4. Formula and Crystallographic Parameters of 3P1CZ Catalyst

	Cordierite high	**Cu_1**	**Cu_1Zr_2**	**O_2Zr_1**	**P_1**
Common name:	Cordierite high	Copper	Zirconium Copper (2/1)	Zirconium Oxide	Phosphorus - A7
Chemical formula:	$Al_4Mg_2O_{18}Si_5$	Cu_1	Cu_1Zr_2	O_2Zr_1	P_1
Crystal system:	Orthorhombic	Cubic	Tetragonal	Orthorhombic	Hexagonal

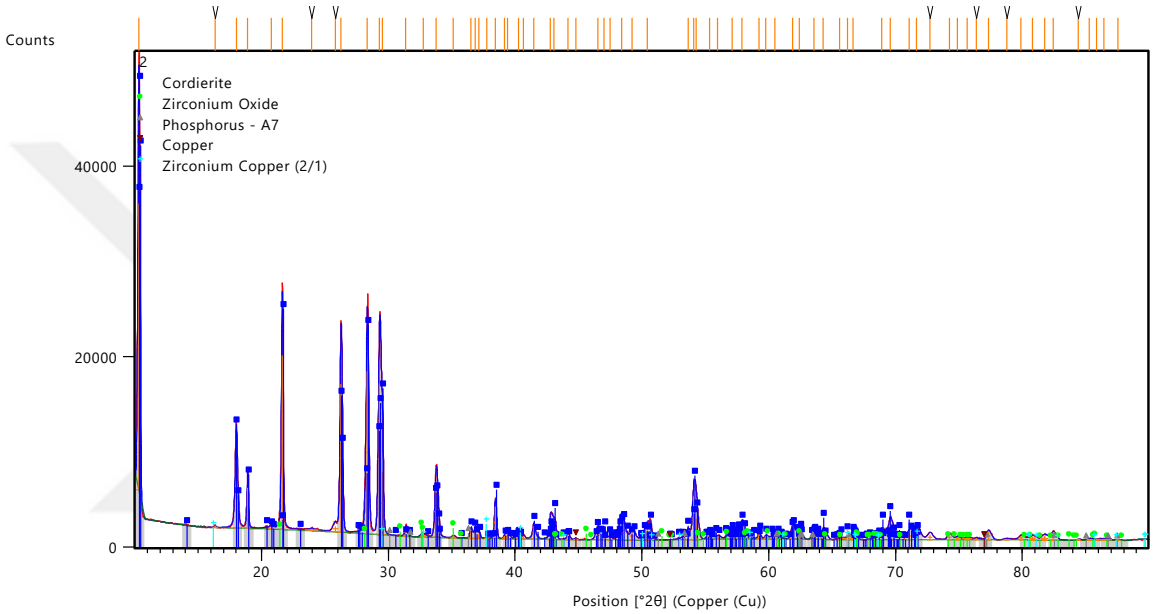

Figure 5.12. XRD analysis of 3P1CZ Catalyst

The XRD analysis for 3P1CZ catalyst shows that, the crystal structure of cordierite ($Al_4Mg_2O_{18}Si_5$) and Zirconium Oxide (O_2Zr_1) was orthorhombic. Copper was in cubic crystal system, Zirconium Copper (2/1) was in orthorhombic structure and Phosphorus (P_1) in hexagonal crystal system. (Table 5.4.)

Figure 5.12. demonstrate the peak values of Cordierite, Zirconium Oxide, Phosphorus-A7, Copper and Zirconium Copper (2/1). Peak points for Cordierite; 2θ = 10.360º, 10.446º, 18.044º, 18.994º, 21.724º, 26.315º, 26.419º, 28.317º, 28.447º, 29.309º, 29.403º, 29.559º, 33.783º, 33.865º. Peak points for Copper; 2θ = 44.816º, 52.23º, 76.997º. Peak points for Zirconium Copper (2/1); 2θ = 37.7º, 40.425º, 58.499º, 66.194º, 71.715º. Peak points for Zirconium Oxide; 2θ = 30.923º, 32.617º, 32.711º, 35.094º, 45.632º, 51.557º, 54.402º, 56.668º, 58.145º, 58.324º, 59.932º, 62.409º, 66.935º, 66.99º, 68.335º. Peak points for Phosphorus - A7; 2θ = 36.343º, 51.286º, 53.379º, 66.296º.

Table 5.5. Formula and Crystallographic Parameters of 2P2CZ Catalyst

	Cordierite high	**Cu_1**	**O_2Zr_1**	**P_1**
Common name:	Cordierite high	Copper	Zirconium Dioxide	Phosphorus - A7
Chemical formula:	$Al_4Mg_2O_{18}Si_5$	Cu_1	O_2Zr_1	P_1
Crystal system:	Orthorhombic	Cubic	Monoclinic	Hexagonal

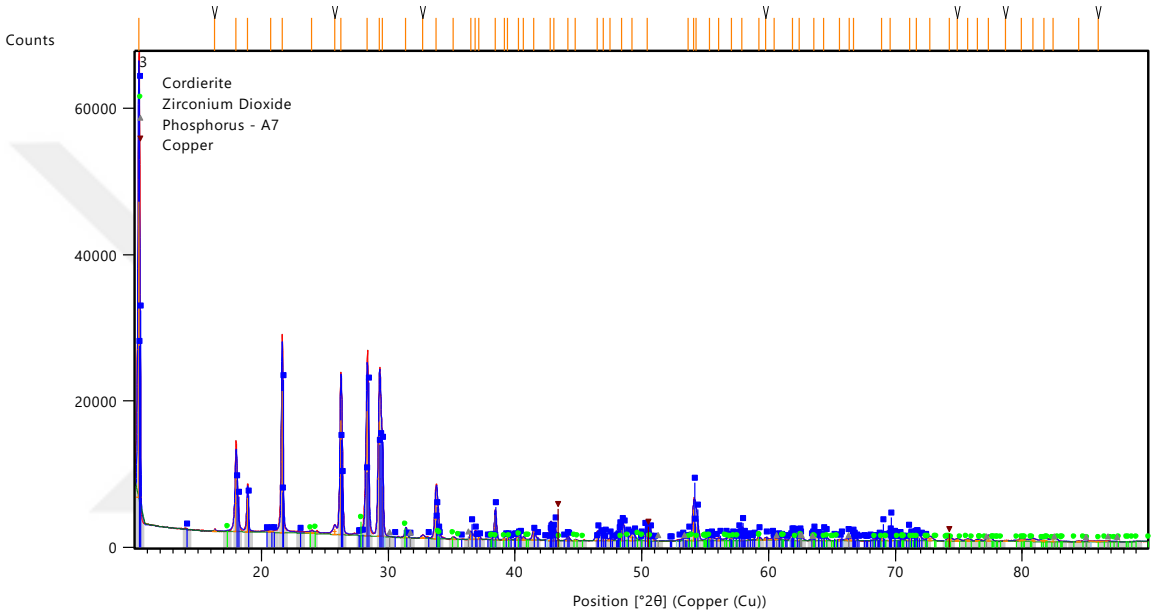

Figure 5.13. XRD analysis of 2P2CZ Catalyst

The XRD analysis for 2P2CZ catalyst shows that, the crystal structure of cordierite ($Al_4Mg_2O_{18}Si_5$) was orthorhombic. Copper was cubic, Zirconium Dioxide in monoclinic crystal system and Phosphorus (P_1) in hexagonal crystal system. (Table 5.5.)

Figure 5.13. demonstrate the peak values of Cordierite, Zirconium dioxide, Phosphorus-A7, and Copper. Peak points for Cordierite; 2θ = 10.370º, 10.459º, 18.063º, 18.217º, 18.976º, 21.671º, 21.714º, 26.315º, 26.423º, 28.319º, 28.454º, 29.332º, 29.430º, 29.592º, 33.881º, 38.499º. Peak points for Copper; 2θ = 43.38º, 50.524º, 74.246º. Peak points for Zirconium Oxide; 2θ = 24.238º, 27.841º, 31.317º, 33.931º, 34.029º, 35.051º, 40.253º, 49.654º, 49.979 º, 53.952º, 55.294º, 62.506º. Peak points for Phosphorus - A7; 2θ = 36.343º, 51.286º, 53.379º, 66.296º.

Table 5.6. Formula and Crystallographic Parameters of 1P3CZ Catalyst

	Cordierite high	**Cu_1**	**Cu_2O_1**	**O_2Zr_1**	**P_1**
Common name:	Cordierite high	Copper	Copper(I) Oxide	Baddeleyite	Phosphorus - A7
Chemical formula:	$Al_4Mg_2O_{18}Si_5$	Cu_1	Cu_2O_1	O_2Zr_1	P_1
Crystal system:	Orthorhombic	Cubic	Cubic	Monoclinic	Orthorhombic

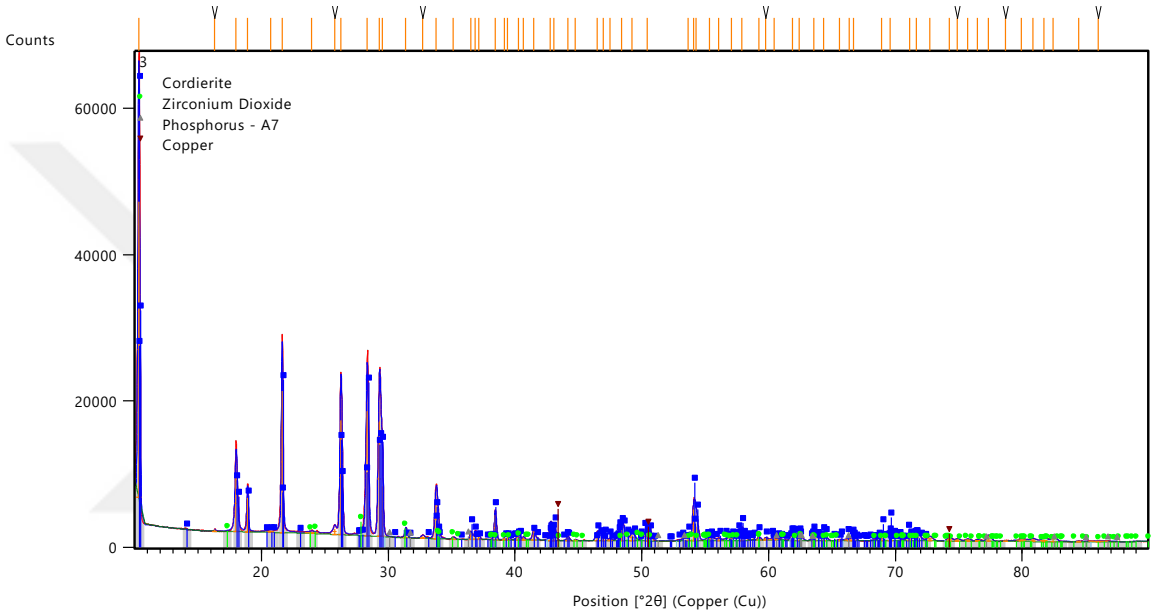

Figure 5.14. XRD analysis of 1P3CZ Catalyst

The XRD analysis for 1P3CZ catalyst shows that, the crystal structure of cordierite and Phosphorus - A7 was orthorhombic. Copper and Copper(I)Oxide were in cubic crystal system and Baddeleyite was in monoclinic structure. (Table 5.6.)

Figure 5.14. demonstrate the peak values of Cordierite, Copper, Copper(I) Oxide, Baddeleyite and Phosphorus - A7. Peak points for Cordierite; 2θ = 10.363º, 10.463º, 18.058º, 18.996º, 21.734, 26.326, 26.448, 28.323, 28.475, 29.323, 29.433, 29.617, 33.796, 38.542, 54.188. Peak points for Copper; 2θ = 43.317º, 50.449º, 74.126º. Peak points for Copper(I) Oxide; 2θ = 36.459º, 42.350º, 61.44º, 73.599º. Peak points for Baddeleyite; 2θ = 24.458º, 28.192º, 31.467º, 34.151º, 34.447º, 35.273º, 40.722º, 50.129º, 50.599º, 54.048º, 59.851º, 62.785º. Peak points for Phosphorus; 2θ = 16.666º, 26.237º, 33.699º, 35.031º, 50.522º, 55.474º, 55.844º, 56.512º, 65.87º.

Table 5.7. Formula and Crystallographic Parameters of 4CZ Catalyst

	Cordierite high	**Cu_1**	**Cu_2O_1**	**O_2Zr_1**
Common name:	Cordierite high	Copper	Dicopper Oxide	Zirconia (nanocrystalline)
Chemical formula:	$Al_4Mg_2O_{18}Si_5$	Cu_1	Cu_2O_1	O_2Zr_1
Crystal system:	Hexagonal	Cubic	Tetragonal	Cubic

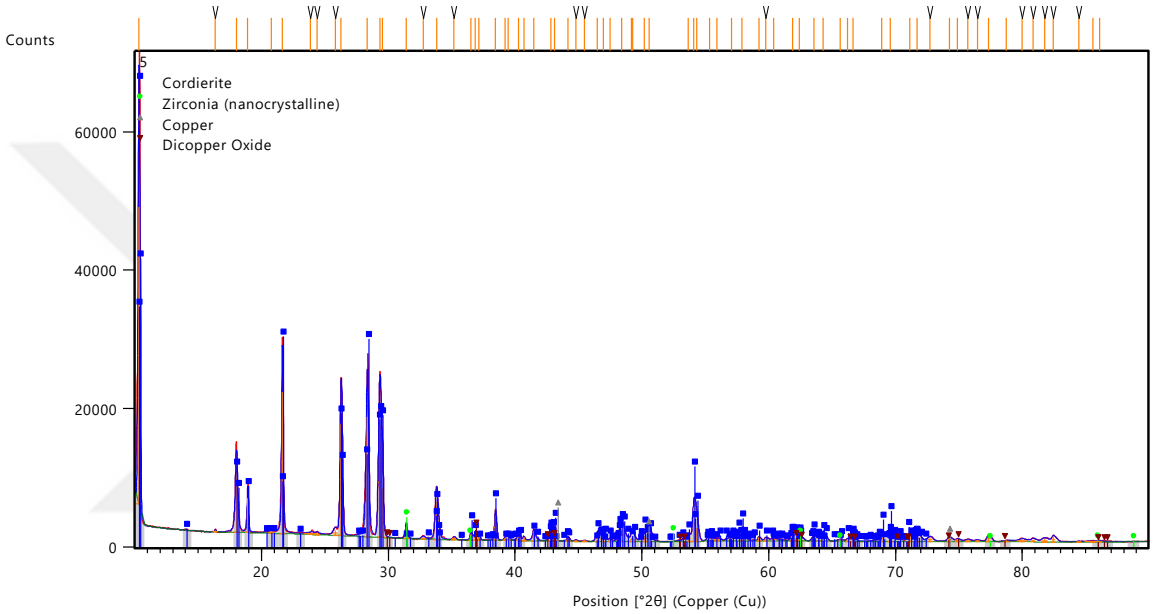

Figure 5.15. XRD analysis of 4CZ Catalyst

The XRD analysis for 4CZ catalyst shows that, the crystal structure of cordierite ($Al_4Mg_2O_{18}Si_5$) was hexagonal. Copper and Zirconia were in cubic crystal system, Dicopper Oxide was tetragonal crystal system. (Table 5.7.)

Figure 5.15. demonstrate the peak values. Peak points for Cordierite; 2θ = 10.37º, 10.459º, 18.063º, 18.217º, 18.976º, 21.671º, 21.714º, 26.315º, 26.423º, 28.319º, 28.454º, 29.332º, 29.43º, 29.592º, 33.881º, 38.499º, 54.162º, 54.398º, 69.661º. Peak points for Copper; 2θ = 43.405º, 50.554º, 74.294º. Peak points for Dicopper Oxide; 2θ = 36.948º, 42.57º, 43.103º, 62.187º, 62.596º, 74.963º. Peak points for Zirconia 2θ = 31.436º, 36.458º, 52.512º, 62.495º.

5.2. NO_x Conversion Rates

This chapter outlines the results of emission tests conducted using the P/ZrO_2, $P\text{-}Cu/ZrO_2$ and Cu/ZrO_2 catalysts in conjunction with ethanol as a reduction agent. The findings demonstrate the impact of temperature, engine load and reductant mixture ratio on NO_x conversion performance.

As evidenced in Table 5.8, high temperatures appear to result in a positive effect on the NO_x conversion ratio. Furthermore, the highest conversion rates for all catalysts were observed when the engine load was at its maximum (4 kW).

Consequently, the average maximum NO_x conversion rate for the 4PZ and 3P1CZ catalysts is almost identical. With regard to the NO_x conversion performance, the order of the catalysts can be stated as follows: 4PZ≈3P1CZ > 2P2CZ > 1P3CZ > 4CZ.

Table 5.8. Average of Maximum NOx Conversion Rates of Catalysts

Catalysts	**Average of Maximum NO_x Conversion Rates (%)**	**Temperature (°C)**	**Engine Load**
4PZ	94,25	230	4 kW
3P1CZ	94,26	240	4 kW
2P2CZ	92,64	240	4 kW
1P3CZ	91,73	240	4 kW
4CZ	91,46	240	4 kW

The following figures (between Figure 5.16. to Figure 5.20.) illustrate the correlation between NO_x conversion rates and temperature. Additionally, the figure presents the engine load factor. For each catalyst, NO_x conversion rate change can be observed within different temperature and engine load parameters. Maximum NO_x conversion rates in Table 5.8. were evaluated by using average of peak values for each test. These peak values were also employed to create figures between Figures 5.16 to Figure 5.20.

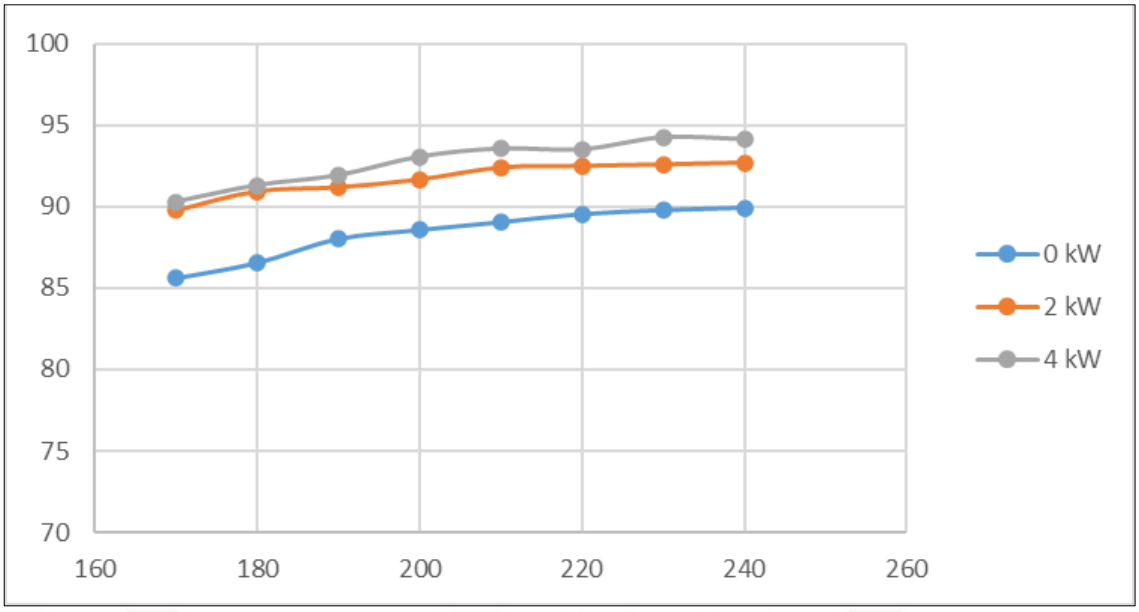

Figure 5.16. NO_x conversion performance at 40000 h^{-1} and 0-2-4 kW for Catalyst 4PZ

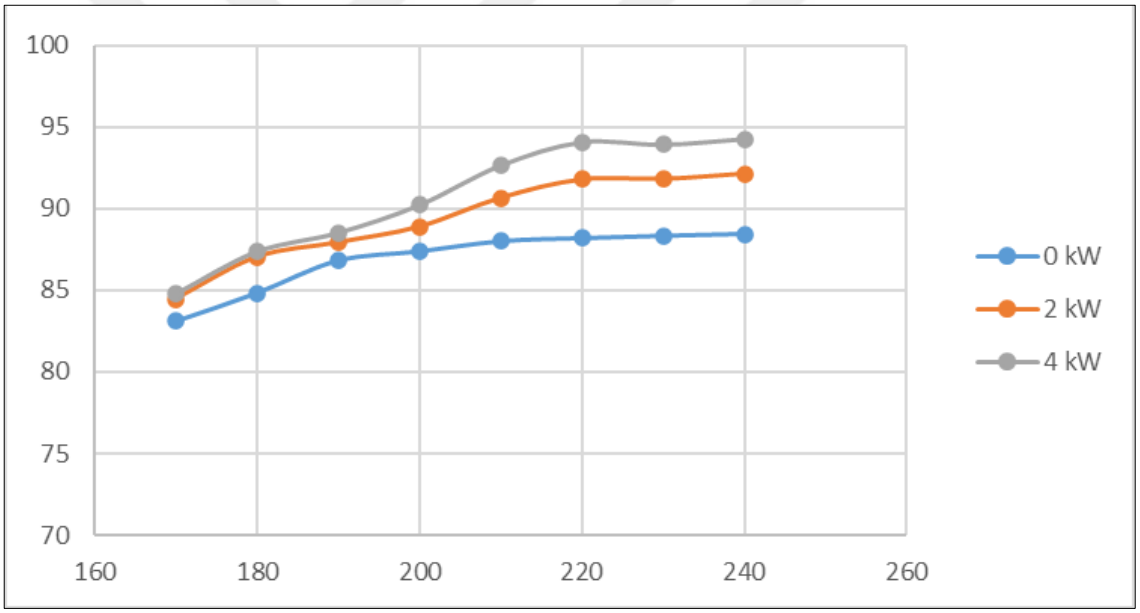

Figure 5.17. NO_x conversion performance at 40000 h^{-1} and 0-2-4 kW for Catalyst 3P1CZ

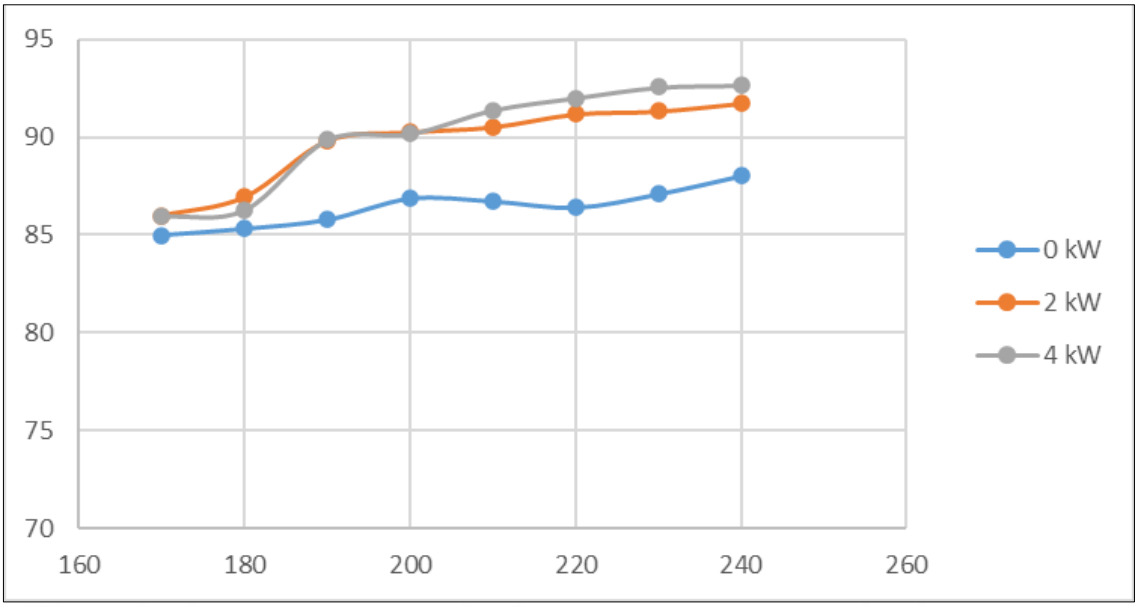

Figure 5.18. NO_x conversion performance at 40000 h^{-1} and 0-2-4 kW for Catalyst 2P2CZ

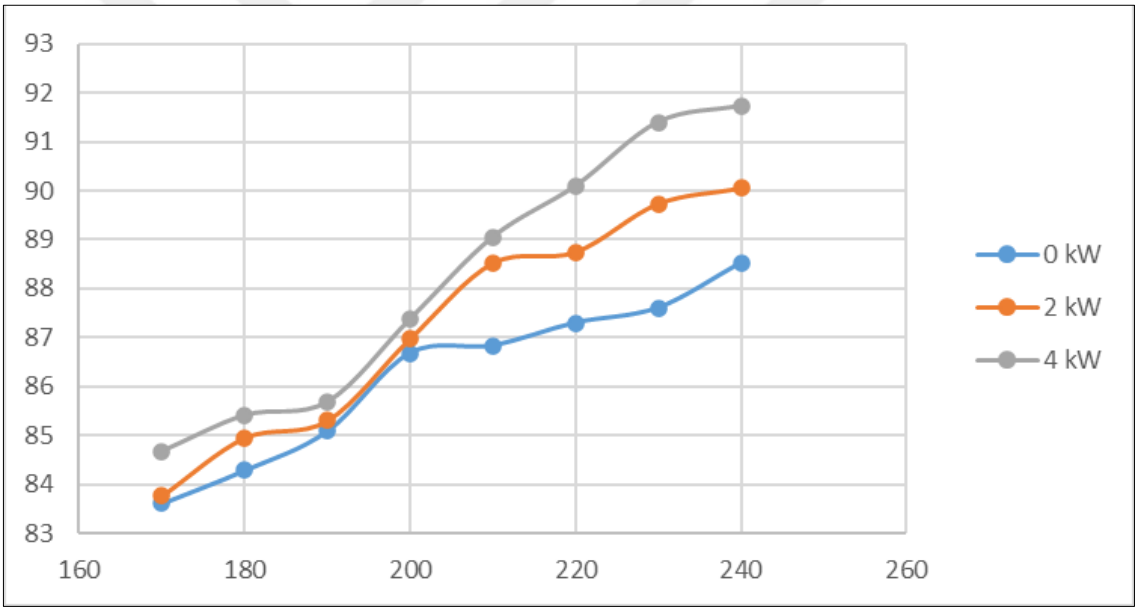

Figure 5.19. NO_x conversion performance at 40000 h^{-1} and 0-2-4 kW for Catalyst 1P3CZ

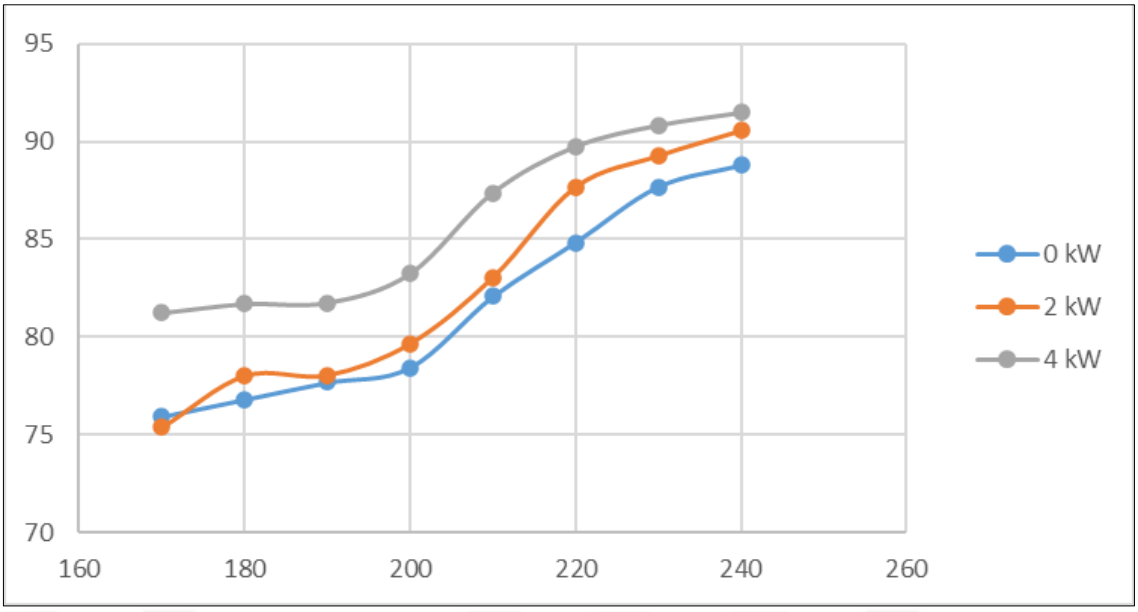

Figure 5.20. NO_x conversion performance at 40000 h^{-1} and 0-2-4 kW for Catalyst 4CZ

5.3. Conclusions

The purpose of this thesis was to ascertain methods of reducing the detrimental emissions generated by diesel engines, which are a significant contributing factor to global warming. Nitrogen oxide (NO_x) is the most significant pollutant emitted from diesel engines. In this thesis, P-Cu/ZrO_2 catalysts were synthesized for an SCR system. Prior to the coating process, the cordierite material was processed with oxalic acid in order to improve the surface characteristics. The catalyst was produced using the impregnation method. Subsequently, the catalysts' s chemical and structural properties were analyzed using SEM, BET, and XRD techniques.

The results of the scanning electron microscopy (SEM) analysis revealed that the porous structure of the cordierite material remained intact throughout the process, and that the coating procedure was successfully completed. The BET analysis revealed a considerable expansion in the surface area of the catalyst following the coating procedure in comparison to the initial surface area of the cordierite material. XRD analysis elucidated the coating process of the coated elements, indicating that they were effectively dispersed over the cordierite surface.

The BET surface area analysis results demonstrate that phosphorus has a more pronounced effect on the enhancement of surface area.

As indicated by the results of the scanning electron microscopy (SEM) analysis, the surface morphology characteristics of the cordierite material can be discerned. Following the application of oxalic acid treatment and coating with various materials, the surface of cordierite exhibits a notable increase in porosity.

In accordance with the EDS results, each material (P, Cu, Zr, Mg O, Si etc.) inside the related catalyst can be observed visually.

The test results demonstrated that the highest temperature provided the optimal conditions for achieving the maximum NO_x conversion rate. Furthermore, the high engine load was identified as a beneficial factor in terms of conversion rate. Almost all catalysts performed better conversion rates with highest temperature 240 °C. Highest conversion rates observed at 4 kW for all of the catalysts. The conversion rates at 4 kW; 4PZ exhibited a near-identical profile when utilizing the 3P1CZ catalyst. A comparative analysis of the maximum NO_x conversion rates of catalysts indicates that they can be ordered as 4PZ≈3P1CZ > 2P2CZ > 1P3CZ > 4CZ. It can be concluded from this order that there was a negative effect on NO_x conversion rates as a result of the decrease in P material and increase in Cu material.

It can be determined that P has a better performance at contribution to NO_x conversion rates according to Cu element.

In consequence of the observed increase in global temperatures, a number of scientific studies have been initiated on a global scale with the objective of reducing NO_x emissions from diesel engines. A notable limitation of research in Turkey is the restricted scope of studies examining diesel exhaust aftertreatment. The findings of this thesis will provide a foundation for future research in diesel exhaust aftertreatment. In future studies, more optimal NO_x conversion results may be achieved by modifying the ratio of elements in the catalyst and the coating method. The influence of modifying the catalyst's physical characteristics and examining the reductant spraying characteristics could also be examined in the context of an SCR system.

REFERENCES

Asghar, U., Rafiq, S., Anwar, A., Iqbal, T., Ahmed, A., Jamil, F., Khurram, M. S., Akbar, M. M., Farooq, A., Shah, N. S., & Park, Y. K., 2021. Review on the progress in emission control technologies for the abatement of CO2, SOx and NO_x from fuel combustion. In Journal of Environmental Chemical Engineering (Vol. 9, Issue 5). Elsevier Ltd. https://doi.org/10.1016/j.jece.2021.106064

Aswin, C. G., Kumareswaran, A., Lakshmanan, R., Mathavan, S., Andal, V., Lakshmipathy, R., & Rico, I. L. R., 2022. Comparative Analysis of NO_x Emission Reduction in Engines Using $NiCO_2O_4$ Nanoparticles without External Reductant at Low Temperatures: An Experimental Investigation. *Journal of Nanomaterials*, *2022*. https://doi.org/10.1155/2022/8981350

Cai, X., Sun, W., Xu, C., Cao, L., & Yang, J., 2016. Highly selective catalytic reduction of NO via SO_2/H_2O-tolerant spinel catalysts at low temperature. *Environmental Science and Pollution Research*, *23*(18), 18609–18620.

https://doi.org/10.1007/s11356-016-7061-y

CeramTec, Low Thermal Conductivity meets High Strength, https://www.ceramtec-industrial.com/en/materials/zirconium-oxide#:~:text=Zirconium%20oxide%20ceramics%20are%20used,measurement%20cells%20in%20lambda%20probes., [accessed: 01.11.2024].

Çalışkan, H. H., 2021. *Çukurova University Institute of Natural and Applied Sciences Msc Thesis Hakan Hanna Çalişkan Use of Ethyl Alcohol – Adblue Mixture As A Reductant Agent in A Scr System at Low Temperature Conditions Department of Automotive Engineering Adana-2021*.

Dieselnet, Diesel Particulate Filters,

https://dieselnet.com/tech/dpf.php, [accessed: 01.11.2024].

Dieselnet, Emission Standards: Europe: Heavy-Duty Truck and Bus Engines, https://dieselnet.com/standards/eu/hd.php, [accessed: 01.11.2024].

EU Commission, Zero Pollution Action Plan, https://environment.ec.europa.eu/strategy/zero-pollution-action-plan_en, [accessed: 01.11.2024].

EUR-Lex, Regulation (EU) 2024/1257, https://eur-lex.europa.eu/eli/reg/2024/1257/oj, [accessed: 01.11.2024].

Hamada, H., & Haneda, M., 2012. A review of selective catalytic reduction of nitrogen oxides with hydrogen and carbon monoxide, Applied Catalysis A: General 421, 1-13.

https://doi.org/10.1016/j.apcata.2012.02.005

He, H., Zhang, C., & Yu, Y., 2004. A comparative study of Ag/Al_2O_3 and Cu/Al_2O_3 catalysts for the selective catalytic reduction of NO by C_3H_6. *Catalysis Today*, *90*(3–4), 191–197. https://doi.org/10.1016/j.cattod.2004.04.026

He, X., Wang, M., jin, T., & Li, L., 2024. Characterization and photocatalytic properties of porous ZrO_2/Al_2O_3 ceramic bead supported BiOI catalyst. *Ceramics International*, *50*(7), 12529–12538.

https://doi.org/10.1016/j.ceramint.2024.01.162

He, Y., Liu, J., Zhang, G., Zang, P., Li, G., & Wang, Y., 2022. Insights into the structure-activity relationships of highly efficient CuCe oxides for the low temperature CO oxidation and CO-SCR. *Journal of the Energy Institute*, *104*, 142–155. https://doi.org/10.1016/j.joei.2022.07.006

He, J., Jiang, Y., Ding, B., Wang, Y., Qiu, H., Dai, S., Zhao, X., & Hou, Z., 2023. Zirconium phosphate supported copper catalyst for selective oxidation of phenol to cis, cis-muconic acid. *Applied Catalysis A: General*, *664*.

https://doi.org/10.1016/j.apcata.2023.119351

Jeguirim, M., Tschamber, V., Brilhac, J. F., & Ehrburger, P., 2005. Oxidation mechanism of carbon black by NO_2: Effect of water vapour. *Fuel*, *84*(14–15), 1949–1956. https://doi.org/10.1016/j.fuel.2005.03.026

Jia, Q., Hu, S., & Liu, Y., 2024. Hydrophobically modified ceramic-supported Pt-particle catalyst for enhanced water–hydrogen exchange reactions. *Fusion Engineering and Design*, *199*. https://doi.org/10.1016/j.fusengdes.2024.114154

Jung, Y., Pyo, Y., Jang, J., Woo, Y., Ko, A., Kim, G., Shin, Y., & Cho, C., 2022. Nitrous oxide in diesel aftertreatment systems including DOC, DPF and urea-SCR. *Fuel*, *310*. https://doi.org/10.1016/j.fuel.2021.122453

Keskin, Z., 2019. Metal Nano Partiküllerin Kullanımı ile Seçici Katalitik İndirgeme Sistemi Tasarlanması ve Test Edilmesi, PhD Thesis, Tarsus University, Tarsus, p. 115.

Keskin, A., & Emiroğlu, A. O., 2016. Catalytic Reduction techniques for post-combustion diesel exhaust emissions. Uluslararası Yakıtlar Yanma ve Yangın Dergisi, (1), 16-21.

Keskin, Z., Özgür, T., Özarslan, H., and Yakaryılmaz, A. C., 2021. Effects of hydrogen addition into liquefied petroleum gas reductant on the activity of Ag–Ti–Cu/Cordierite catalyst for selective catalytic reduction system. *International Journal of Hydrogen Energy*, *46*(10), 7634-7641.

Kim, S. C., 2002. The catalytic oxidation of aromatic hydrocarbons over supported metal oxide. *Journal of Hazardous Materials, 91*(1-3), 285-299.

Lakshminarayanan, P. A., Kumar, A., 2020. Design and Development of Heavy Duty Diesel Engines, Springer, p. 912.

http://www.springer.com/series/15901

Matti Maricq, M., 2007. Chemical characterization of particulate emissions from diesel engines: A review. *Journal of Aerosol Science* (Vol. 38, Issue 11, pp. 1079–1118). Elsevier Ltd. https://doi.org/10.1016/j.jaerosci.2007.08.001

Özarslan, H., 2022. Hybrid Catalyst Synthesis and Performance Characteristics For Selective Catalytic Reduction Systems, Çukurova University, MSc Thesis, Adana, p. 137.

Özarslan, H., and Keskin, A., 2022. Enhancement of Surface Area of Cordierite Structure by Oxalic Acid Treatment for SCR Applications. *Çukurova Üniversitesi Mühendislik Fakültesi Dergisi*, *37*(1), 33–41.

https://doi.org/10.21605/cukurovaumfd.1094938

Pan, K. L., Young, C. W., Pan, G. T., and Chang, M. B., 2020. Catalytic reduction of NO by CO with Cu-based and Mn-based catalysts. *Catalysis Today*, *348*, 15–25. https://doi.org/10.1016/j.cattod.2019.08.038

Pulkrabek, W. W., 1997. Engineering Fundamentals of the Internal Combustion Engine. Prentice Hall, Upper Saddle River. p. 426.

Reşitoğlu, I. A., 2016. Dizel Motorlarda Kirletici Emisyonların Kontrol Edilmesine Yönelik Fe_2O_3 Esaslı Katalizörlerin Kullanıldığı DOC ve SCR Sistemlerinin Geliştirilmesi. Selçuk Üniversitesi, Konya, p. 123.

Reşitoğlu, I. A., Altinişik, K., and Keskin, A., 2015. The pollutant emissions from diesel-engine vehicles and exhaust aftertreatment systems. Clean Technologies and Environmental Policy, 17, 15–27.

https://doi.org/10.1007/s10098-014-0793-9

Sarvi, A., Lyyränen, J., Jokiniemi, J., and Zevenhoven, R., 2011. Particulate emissions from large-scale medium-speed diesel engines: 1. Particle size distribution. Fuel Processing Technology, *92*(10), 1855–1861.

https://doi.org/10.1016/j.fuproc.2011.04.031

Sawatmongkhon, B., 2011. Modeling of Catalytic Aftertreatment of NO_X Emissions Using Hydrocarbon As A Reductant, PhD Thesis, University of Birmingham.

http://etheses.bham.ac.uk/3138/1/Sawatmongkhon12PhD.pdf

Seneque, M., Courtois, X., Can, F., and Duprez, D., 2016. Direct Comparison of Urea-SCR and NH_3-SCR Activities Over Acidic Oxide and Exchanged Zeolite Prototype Powdered Catalysts. Topics in Catalysis, 59, 938–944.

https://doi.org/10.1007/s11244-016-0572-4ï

Shan, Y., Sun, Y., Du, J., Zhang, Y., Shi, X., Yu, Y., Shan, W., and He, H., 2020. Hydrothermal aging alleviates the inhibition effects of NO_2 on Cu-SSZ-13 for NH_3-SCR. Applied Catalysis B: Environmental, 275., 119105.

https://doi.org/10.1016/j.apcatb.2020.119105

Shiyu, L., Boyuan, W., Zexian, G., Buyu, W., Zhaohuan, Z., Xiao, M., Chen-Teng, C., Peng, W., Xin, H., Xingyu, S., and Shijin, S., 2022, Experimental investigation of urea injection strategy for close-coupled SCR aftertreatment system to meet ultra-low NO_x emission regulation, Applied Thermal Engineering, 205, 117994.
https://doi.org/10.1016/j.applthermaleng.2021.117994

Wang, Y., Zhang, M., Du, Y., Cao, L., and Wang, W., 2024. Magnesium borate whiskers/La2-XCeXZr$_2$O$_7$ catalysts preparation on cordierite honeycomb ceramic surfaces for soot catalytic oxidation. Ceramics International, Volume 50, Issue 17, Part B, 31124–31134. https://doi.org/10.1016/j.ceramint.2024.05.418

Wang, F., Yuan, Z., Liu, B., Chen, S., and Zhang, Z., 2016. Catalytic oxidation of biomass derived 5-hydroxymethylfurfural (HMF) over RuIII-incorporated zirconium phosphate catalyst. Journal of Industrial and Engineering Chemistry, 38, 181–185. https://doi.org/10.1016/j.jiec.2016.05.001

Yamada, H., Misawa, K., Suzuki, D., Tanaka, K., Matsumoto, J., Fujii, M., and Tanaka, K., 2011. Detailed analysis of diesel vehicle exhaust emissions: Nitrogen oxides, hydrocarbons and particulate size distributions, Proceedings of the Combustion Institute, *33*(2), 2895–2902. https://doi.org/10.1016/j.proci.2010.07.001

Zhang, Y., Wang, X., Mao, Y., Song, C., Zhang, Z., and Zheng, W., 2024. Revealing the reaction regularity of Mn-CeO2-x catalyst system in catalytic filter for low-temperature NH3-SCR, Journal of Industrial and Engineering Chemistry, *136*, 222–228. https://doi.org/10.1016/j.jiec.2024.02.009

Zhang, W., Zhang, Z., Chen, H., Ji, Z., Ma, Y., and Sun, F., 2024. A review on performance, combustion and emission of diesel and alcohols in a dual fuel engine, Journal of the Energy Institute (Vol. 116), Elsevier B.V.
https://doi.org/10.1016/j.joei.2024.101760

Zhang, Z., Li, D., Lan, G., Yin, Z., Pan, M., Jiang, F., Li, J., and Tan, D., 2024. Development and evaluation of mechanistic model for standard SCR, fast SCR, and NO2 SCR of NH3-SCR over Cu-ZSM-5, Energy, 306.
https://doi.org/10.1016/j.energy.2024.132544

Zheng, M., and Banerjee, S., 2009. Diesel oxidation catalyst and particulate filter modeling in active - Flow configurations, Applied Thermal Engineering, 29(14–15), 3021–3035. https://doi.org/10.1016/j.applthermaleng.2009.04.017

CURRICULUM VITAE

Eylem Özgün, Following the completion of her education at Mersin Yusuf Kalkavan Anatolian High School, she proceeded to enroll in the Automotive Engineering Department at Cukurova University in 2012 and graduated in 2017. She has been working as Homologation Engineer since 2018.